ИНСТИТУТ ЯДЕРНОЙ ФИЗИКИ
им. Г.И. Будкера СО РАН

M.M. Karliner, N.V. Mityanina, V.P. Yakovlev

THE IMPEDANCE OF A TOROIDAL CHAMBER WITH WALLS OF FINITE CONDUCTIVITY. WAVEGUIDE MODEL

BUDKERINP 93-90

НОВОСИБИРСК

The Impedance of a Toroidal Chamber with Walls of Finite Conductivity. Waveguide Model.

M.M.Karliner, N.V. Mityanina, V.P. Yakovlev.

Abstract

Using the waveguide model, we study the longitudinal coupling impedance in a toroidal chamber with walls of finite conductivity. At high frequencies the beam can excite in the chamber resonant modes with the phase velocity equal to the particle velocity due to a delay because of curvature and resistance. The longitudinal impedance, as a function of the azimuthal harmonic number, has relatively broad peaks. Admitting that the excited fields damp during one turn, that usually takes place even in the mashines with small radius, we propose to spread the excited field over the eigen functions of the curved waveguide instead of azimuthal harmonics, as when applying the cavity model. It enables us to get the expression for impedance in the form, which can be easy compared with the straight waveguide; to describe every resonance with the only term of the expansion; to get the contribution due to the curvature summing up comparatively small number of terms. We have got the accurate results separately for finite conductivity of vertical and horizontal walls; in the resonant region, we can take into account simultaneously the finite conductivity of all four walls. The results are generalized on the case of non-circular storage ring, for which the impedance can be calculated separately for every segment with constant curvature. The finite radial dimension of the electron beam also can be easy taken into account. The estimation formulae for parameters of resonances are given at the conclusion.

1. INTRODUCTION

We study the fields produced by an arbitrary particle beam in a toroidal chamber with walls of finite conductivity and rectangular cross section.

Some authors paid attention to this problem ([1] - [3]) calculating a coupling impedance $Z(n,\omega)$ (n is azimuthal harmonic number). The common feature of these works is using the resonator base for derivations of electromagnetic field in the chamber; the field and a beam current being spread over azimuthal harmonics.

The longitudinal impedance $Z(n,n\omega_0)/n$ (ω_0 - a revolution frequency), as a function of the azimuthal harmonic number n, has relatively broad peaks. Therefore, calculating the impedance in the resonant region, one should sum up a great number of terms with harmonic numbers within the resonant band.

Unlike this way, we prefer to use the waveguide base when studying the resistive impedance of a toroidal chamber. We can use this base, when the fields excited by the beam damp to zero in one turn due to the chamber walls finite conductivity, that usually takes place even in the mashines with small radius. Being more natural for such cases, it appears to produce more convenient expression for the impedance in a form analogous to the straight waveguide, which has some advantages. So, near the resonances, the impedance is described by the only main term. Further, if we would take into account the radial dimension of the beam, we can average over the cross section only the resonant factor having a simple form.

As we pretend on an accurate solution, we take into account the coupling of TE and TM modes due to the Leontovich boundary conditions on the walls of finite conductivity. The conditions on vertical and horizontal walls cannot be satisfied simultaneously for the coupled modes, that's why we consider at first these conditions separately. However, in the resonant region, the main

contribution is made by the "delayed" modes, which are practically uncoupled, thus, the impedance in the resonant regions can be calculated correctly, with the account of finite conductivity of all four walls. The results obtained for the last case are similar to the results of [1].

It seems also possible to use our derivations for non-circular storage rings with sufficient difference of the average ring radius and the local orbit radius in the bending magnets: the impedance can be calculated here separately for every segment with constant curvature.

The estimation formulas for parameters of resonances (resonant frequency, resonant band and shunt resistance) are given at the conclusion.

2. EIGEN FUNCTIONS FOR A CURVED WAVEGUIDE

In this section, we introduce main denotations and consider the functions to be applied further as a basis for expanding the field excited in the chamber by the beam current.

2.1. Denotations.

We consider a toroid of a rectangular cross-section (fig.1), with the inner (outer) radius a (b) and a height h=2g. We use the cylindrical coordinates r=(r,θ,z).

Discussing the chamber with walls of finite conductivity, we will sometimes compare the results for curved and straight waveguide with the same cross section. We will use for a straight waveguide the Cartesian coordinates (x, y, z), corresponding to (r, θ, z) for the curved waveguide (x and r determine the transverse horizontal direction; y and θ - longitudinal; z - vertical).

The eigen modes of the electromagnetic field with a time dependence exp(-iωt) have a form:

$$H_z(r,t)=\sum_{p,l} H_{zpl}(r,\nu,\omega)\sin(k_{zp}(z+g))\,\exp(i\nu\theta-i\omega t), \qquad (2.1)$$

$$E_z(r,t)=\sum_{p,l} E_{zpl}(r,\nu,\omega)\cos(k_{zp}(z+g))\,\exp(i\nu\theta-i\omega t), \qquad (2.2)$$

where $k_{zp}=\pi p/2g$ is the wave number in z-direction, ν is the wave number in θ-direction. The other field components can be expressed via z-components as, for example, [6]:

$$\vec{E}_{pl}=ik\,\mathrm{rot}\vec{\Phi}_{pl}+\vec{\nabla}\mathrm{div}\vec{\Psi}_{pl}+k^2\vec{\Psi}_{pl},\quad Z_0\vec{H}_{pl}=-ik\,\mathrm{rot}\vec{\Psi}_{pl}+\vec{\nabla}\mathrm{div}\vec{\Phi}_{pl}+k^2\vec{\Phi}_{pl}, \qquad (2.3)$$

$$\vec{\Phi}_{pl}=E_{zpl}\vec{e}_z/\gamma_p^2,\quad \vec{\psi}_{pl}=Z_0H_{zpl}e_z/\gamma_p^2, \qquad (2.4)$$

$k=\omega/c$, $\gamma_p^2=k^2-k_{zp}^2$.

2.2. Bessel functions cross-products as eigen functions of the problem.

From the Maxwell equations, we get the equations for E_{zpl}, H_{zpl}:

$$\frac{1}{r}\frac{\partial}{\partial r}\left(r\frac{\partial}{\partial r}\begin{Bmatrix}E\\H\end{Bmatrix}_{zpl}\right)+\left(\gamma_p^2-\frac{\nu^2}{r^2}\right)\begin{Bmatrix}E\\H\end{Bmatrix}_{zpl}=0\,. \qquad (2.5)$$

The general solution of (2.5) is a linear combination of $J_\nu(\gamma_p r)$ and $Y_\nu(\gamma_p r)$.

The boundary conditions (for the infinite walls conductivity) at r=a,b are:

$$E_z\big|_{r=a,b}=0,\quad \frac{\partial}{\partial r}H_z\big|_{r=a,b}=0. \qquad (2.6)$$

Thus, if we use the Bessel functions cross-products (according to [4]):

$$p_\nu(x,y)=J_\nu(x)\,Y_\nu(y)-J_\nu(y)\,Y_\nu(x),$$

$q_\nu(x,y) = \partial p_\nu(x,y)/\partial y$, $r_\nu(x,y) = \partial p_\nu(x,y)/\partial x$,

$s_\nu(x,y) = \partial^2 p_\nu(x,y)/(\partial x \partial y) = \partial q_\nu(x,y)/\partial x$, (2.7)

then the solutions $E_z = p_\nu(\gamma_p r, \gamma_p a)$ and $H_z = q_\nu(\gamma_p r, \gamma_p a)$ satisfy the zero boundary conditions at the inner radius a; the conditions at the outer radius b determine the eigen value ν, the order of Bessel functions:

$p_\nu(\gamma_p b, \gamma_p a)=0$ (for E_z, or TM, modes),

$s_\nu(\gamma_p b, \gamma_p a)=0$ (for H_z, or TE, modes).

The eigen values, gotten from the boundary conditions for E_z and H_z, due to the curvature of the waveguide, do not coincide, thus the set of eigen modes splits on the set of TE modes, with $E_z = 0$, $H_z \neq 0$, and the set of TM modes, with $E_z \neq 0$, $H_z = 0$.

The order of Bessel functions, being the eigen value of the problem, unlike the way of expansion over azimuthal harmonics([1]-[3]), is not integer, and moreover, in the case of the finite walls conductivity, is a complex number with a small imaginary part. The Bessel function $Z_\nu(x)$ of a complex order $\nu=\nu_1+i\nu_2$, $\nu_2 \ll \nu_1$, will be calculated via the function of real order and their order-derivatives as

$$Z_\nu(x) = Z_{\nu_1}(x) + i\nu_2 \frac{\partial}{\partial \nu} Z_{\nu_1}(x). \qquad (2.8)$$

In [4], the order derivatives of Bessel functions are given as infinite series, not quite convenient for calculations. But as for Bessel functions of great order we will use further the approximate formulas, we will derive these formulas instead of summing the series.

Consider some typical features of the eigen functions. As we can see, the arguments and the order of functions

$p_\nu(x_1,x_2)$, $q_\nu(x_1,x_2)$ are rather great numbers; depending on the order ν, these functions differ essentially in two cases:

a) $\nu<x_1<x_2$.

The functions $p_\nu(x,x_2)$, $q_\nu(x,x_2)$ $(x_1<x<x_2)$ resemble the ordinary eigen functions of straight waveguide sine and cosine; the less ν and the more the arguments, the nearer these functions to the trigonometric.

b) $x_1<\nu<x_2$.

The functions $p_\nu(x,x_2)$, $q_\nu(x,x_2)$, with $x_1<\nu<x_2$ in the interval $x_1<x<x_2$ look rather unsymmetrically: at $x_1<x<\nu$ the functions behavior is approximately exponential, and at $\nu<x<x_2$ - sine-shaped (with uniformly changing amplitude).

Fig.2 shows the typical of the functions p_ν, q_ν, s_ν for the second case. Note that the amplitude of p_ν decreases, and the amplitude of s_ν increases when the first argument increases. That leads to the opposite signs of the contribution to the impedance due to the curvature for TE and TM modes, as will be seen further.

3. DERIVATIONS OF THE IMPEDANCE

3.1. A field induced by a beam.

A field induced by a beam current with a density $\vec{j}_\omega$ ([6]) can be written as

$$\vec{E} = \vec{E}_1 + \vec{E}_2, \qquad (3.1)$$

$$\vec{E}_1 = \sum_s \left(C_s \vec{E}_s + \vec{C}_{-s} \vec{E}_{-s} \right), \quad \vec{E}_2 = \frac{1}{i\omega\varepsilon} j_\omega, \qquad (3.2)$$

$$C_{\pm s}=\frac{1}{N_{\pm s}}\int_{-\infty(l)}^{l(+\infty)}\vec{j}_{\omega}\,\vec{E}_{\mp s}d\vec{r}\,,\qquad N_s=2\int[\vec{E}\times\vec{H}]d\vec{r}_{\perp}. \tag{3.3}$$

Here the index $\pm s$ denotes the modes expanding in the positive or negative propagation direction, l is the current coordinate in this direction; $\int d\vec{r}$ means integration over the space; $\int d\vec{r}_{\perp}$ means integration over the cross section of the waveguide; $\vec{E}_{\mp s}$ are the eigen fields of the waveguide.

By the way, we must note that at calculating N_s for a toroidal chamber there appear the integrals of p_ν^2, q_ν^2 and $p_\nu q_\nu$ over this chamber cross section. The expressions of these integrals via the order-derivatives of the Bessel functions is given in App.1.

The second term in (3.1) gives the purely imaginary not resonant contribution into the impedance and is not changed when we take into account the finite wall conductivity. As our main interest in this paper is the real part of the impedance and the resonant behavior of the impedance, we will not mention this term further (but if one is interested in the imaginary part of the impedance, he must add the second term).

3.2. A beam model.

We consider now the beam current analogously to [1], a beam with finite width in z-direction and delta-function distribution in r-direction (in the last section we will discuss a possibility to take into account the finite r-dimension of the beam). The charge density of the current is

$$\rho(r,\theta,z,t) = q\,\lambda(\theta-\omega_0 t)H(z)W(r); \tag{3.4}$$

$$\int_0^{2\pi}\lambda(\theta)d\theta = 1;\quad \int_{-g}^{g}H(z)dz = 1;\quad \int_a^b W(r)r\,dr = 1. \tag{3.5}$$

We consider now a rectangular z-distribution and delta-function r-distribution (the beam with nonzero radial dimension will be discussed further):

$$W(r)=\delta(r-R)/R; \tag{3.6}$$

$$H(z)=\frac{1}{\delta h}\begin{cases}1, & |z-z_0|\le\delta h/2\,,\\ 0, & |z-z_0|>\delta h/2\,;\end{cases} \tag{3.7}$$

Here R is the radial position of the beam; z_0 is z-position of the beam center; δh is its z-dimension; ω_0 is the frequency of the beam revolution:
$\omega_0=\beta c/R=\beta c k_0$, $\beta=v/c$, v - the beam velocity.

The longitudinal component of the current density is

$$j_\theta(r,\theta,z,t) = \beta c q\,\rho(r,\theta,z,t)\frac{r}{R}, \tag{3.8}$$

with a Fourier transformation

$$j_\omega(r,\theta,z)=\frac{1}{2\pi}\int_{-\infty}^{+\infty}j_\theta(r,\theta,z,t)e^{-i\omega t}dt =$$

$$= q\,r\,H(z)W(r)\tilde{\lambda}(\omega/\omega_0)\,e^{-i\theta\omega/\omega_0}, \tag{3.9}$$

where $$\tilde{\lambda}(\nu) = \int_{-\infty}^{+\infty}\lambda(\theta)\,e^{-i\nu\theta}d\theta. \tag{3.10}$$

3.3. The impedance derivation.

Denoting

$$H_p = \frac{1}{g}\int H(z)\sin(k_{zp}z+\pi p/2)\,dz = \sin(k_{zp}z_0)\sin(k_{zp}\delta h/2)/(k_{zp}g), \tag{3.11}$$

we can write

$$C_{\pm s} = \frac{1}{N_{\pm s}}\, q\,\tilde{\lambda}(\omega/\omega_0)H_p g\,\frac{\exp(-i(\omega/\omega_0 \pm \nu)\theta)}{i(\omega/\omega_0 \pm \nu)} R\,E_{\pm s,\theta}(R,\omega), \tag{3.12}$$

where the index s denotes the eigen mode number. Note that in (3.12) we have omitted the dependence of the longitudinal wave number ν on the frequency ω and the mode number s.

Now we can write the longitudinal field induced by the beam:

$$E_{1\theta}(r,\theta,z,\omega) = \sum_s \frac{q\tilde{\lambda}(\omega/\omega_0)H_p gR}{iN_s}\,\frac{2\nu}{(\omega/\omega_0)^2-\nu^2}\,e^{-i\theta\omega/\omega_0}\times$$
$$\times E_{s,\theta}(R,\omega)\,E_{s,\theta}(r,\omega)\,\sin(k_{zp}z+\pi p/2). \tag{3.13}$$

Averaging the longitudinal field over the cross section of the beam, we determine the impedance as

$$-2\pi R\langle E_{1,\theta}\rangle = Z(\omega)\,I_\theta(\omega), \tag{3.14}$$

where $I_\theta(\omega) = \int j_\omega d\vec{r}_\perp = q\,\tilde{\lambda}(\omega/\omega_0)e^{-i\theta\omega/\omega_0}$.

Putting (3.13) into (3.14), we get

$$Z_1(\omega) = -2\pi R^2 \sum_s \frac{\Lambda_p}{iN_s}\,\frac{2\nu}{(\omega/\omega_0)^2-\nu^2}\,E^2_{s,\theta}(R)\sin^2(k_{zp}z_0+\frac{\pi p}{2}), \tag{3.15}$$

or, introducing the azimuthal harmonic number $n=k/k_0$, $k=\omega/c$,

$k_0 = 1/R$,

$$\frac{Z_1(\omega)}{n} = -\frac{2\pi}{k}\sum_s \frac{\Lambda_p}{iN_s}\,\frac{2\nu R}{(\omega/\omega_0)^2-\nu^2}\,E^2_{s,\theta}(R)\sin^2(k_{zp}z_0+\frac{\pi p}{2}). \tag{3.16}$$

Here we have denoted

$$\Lambda_p = \left(\frac{\sin(\alpha_p \delta h/2)}{\alpha_p \delta h/2}\right)^2. \tag{3.17}$$

3.4. Comparison with the straight waveguide.

As can be easy shown, for the straight waveguide we have the analogous expression:

$$\frac{Z'_1(\omega)}{n} = -\frac{2\pi}{k}\sum_s \frac{\Lambda_p}{iN'_s}\,\frac{2k_y}{(k/\beta)^2-k_y^2}(E'_{s,y}(R)\sin(k_{zp}z_0+\frac{\pi p}{2}))^2, \tag{3.18}$$

where the axis y denotes the longitudinal direction, and ' marks the modes of a straight waveguide.

3.5. Remarks.

We must make here two remarks concerning the impedance $Z_1(\omega)$.

1) $Z_1(\omega)$ represents only one term of the full impedance; the full impedance we can get taking into account the second term of the induced electric field, $\vec{E}_2$ (3.2). For the straight waveguide with infinite walls conductivity it leads to the well known factor $1/\gamma^2$:

$$E_y = E_{1,y} + E_{2,y} = E_{1,y} - E_{1,y}\frac{1}{\beta} = -\frac{1}{2\gamma^2}E_{1,y}.$$

2) We will consider further only the term $Z_1(\omega)$ because

a) we are interested mainly in the real part of the impedance, and the second term is purely imaginary (the imaginary part of the impedance can be determined, if the frequency dependence of the real part is known), and

b) we are interested the contribution to the real part of the impedance due to the curvature, that is the difference between Z and Z′.

As, at increasing the vertical and radial modes number, this difference tends to zero, we can limit the number of modes to be calculated, and moreover, the non-spreading modes with imaginary longitudinal wave number also can be omitted. It saves us from the necessity to calculate the Bessel functions of imaginary order and of small real order. Thus, at calculations, we can use the only approximation of Bessel functions for big order and arguments.

4. EIGEN VECTORS FOR FINITE CONDUCTIVITY WALLS

In this section, we will derive the electromagnetic field eigen modes for the chamber with walls of finite conductivity.

4.1. The boundary conditions.

The Leontovich boundary conditions on the walls of finite conductivity have a form:

$$\left.\begin{aligned} E_y &= \mp i\eta Z_0 H_z \,, \\ E_z &= \pm i\eta Z_0 H_y \,, \end{aligned}\right\} \quad x = d,\ 0 \quad (\text{or } r = b,\ a) \qquad (4.1),\ (4.2)$$

$$\left.\begin{aligned} E_y &= \pm i\eta_z Z_0 H_x, \\ E_x &= \mp i\eta_z Z_0 H_y, \end{aligned}\right\} \quad z = g,\ -g \qquad (4.3),\ (4.4)$$

where $\eta = (1+i)\sqrt{k/(\sigma Z_0)}$; $\eta_z = (1+i)\sqrt{k/(\sigma_z Z_0)}$; σ and σ_z are the conductivities of the vertical and horizontal walls.

In the case of a straight waveguide, these conditions lead to the splitting of the degenerated eigen modes on E_x and H_x modes (i.e. the modes with $E_x \neq 0$, $H_x = 0$ and $E_x = 0$, $H_x \neq 0$ correspondingly) for finite conductivity of vertical walls or on E_z and H_z modes (analogously) for finite conductivity of horizontal walls.

When we try to find the eigen modes of a waveguide with all four walls of finite conductivity, it appears that all boundary conditions cannot be satisfied simultaneously, because they are not persistent. Thus, we can get the accurate solution only for a couple of walls of finite conductivity - horizontal or vertical.

For a straight waveguide, the boundary conditions on the vertical walls (4.1) and (4.2) lead to the dispersion relation

$$\mathrm{tg}(k_x d/2) = -\eta \left(\frac{k}{k_x}\right)^{\pm 1} \quad \text{for } E_x\ (H_x) \text{ modes.} \qquad (4.5)$$

Analogously, the boundary conditions on the horizontal walls (4.3) and (4.4) lead to the dispersion relation

$$\mathrm{tg}(k_z g) = -\eta_z \left(\frac{k}{k_z}\right)^{\pm 1} \quad \text{for } E_z\ (H_z) \text{ modes.} \qquad (4.6)$$

As for the curved waveguide, the curvature without finite conductivity splits the eigen modes on E_z and H_z modes. The boundary conditions (4.3) and (4.4) retain this splitting and lead to the dispersion relation (4.6). But in the case of finite conductivity of vertical, curved walls, the counteraction of two effects can lead to different results.

If the curvature effect is weak as compared with the

conductivity, the modes E_z and H_z are coupled and form the modes analogous to E_x and H_x of the straight waveguide. (Due to the curvature, in the mode analogous to E_x (H_x), the field component H_r (E_r) is not exactly zero, so, it is not "pure" E_r (H_r) mode.)

In the opposite case, if the curvature effect prevails, coupling of E_z and H_z modes is weak, and the eigen modes of the curved waveguide differ essentially from modes of the straight one. Note that a measure of curvature is a comparison of orders and arguments of Bessel functions describing the toroidal waveguide eigen modes: small orders (as compared with arguments) correspond to the modes slightly distinguishing from the straight waveguide modes; and contrary, the modes with orders near to the arguments can have essential differences.

4.2. The vertical walls of finite conductivity.

Now we will calculate the eigen modes of the toroidal waveguide with the vertical walls of finite conductivity. The boundary conditions (4.1) and (4.2) instead of (2.6) lead to the necessity to search the eigen modes in a form:

$$E_{zpl} = A\, p_\nu(\gamma_p r,\gamma_p a) + B\, q_\nu(\gamma_p r,\gamma_p a), \qquad (4.7)$$

$$H_{zpl} = C\, p_\nu(\gamma_p r,\gamma_p a) + D\, q_\nu(\gamma_p r,\gamma_p a). \qquad (4.8)$$

Denoting

$$\varepsilon = k/\gamma_p;\ \xi_a = k_{zp}\nu/(\gamma_p^2 a);\ \xi_b = k_{zp}\nu/(\gamma_p^2 b);\ \beta_{a,b}=(1+\xi_{a,b}^2)/\varepsilon;$$

$$P = p_\nu(\gamma_p b,\gamma_p a)/q_\nu(\gamma_p b,\gamma_p a);\ S = s_\nu(\gamma_p b,\gamma_p a)/q_\nu(\gamma_p b,\gamma_p a);$$

$$\rho = - r_\nu(\gamma_p b,\gamma_p a)/q_\nu(\gamma_p b,\gamma_p a); \qquad (4.9)$$

we can write the boundary conditions neglecting the terms of

$O(\eta^3)$ in a form:

$$\begin{pmatrix} 0 & \xi_a & -\varepsilon & \eta \\ \eta\varepsilon & 1 & 0 & -\eta\xi_a \\ \xi_b P & (\xi_b-\rho\xi_a) & 0 & \varepsilon S-\eta(1+\rho) \\ P-\eta\varepsilon(\rho+1) & 0 & 0 & \eta(\xi_a+\xi_b) \end{pmatrix} \begin{pmatrix} A \\ B \\ C \\ D \end{pmatrix} = \begin{pmatrix} 0 \\ 0 \\ 0 \\ 0 \end{pmatrix}. \qquad (4.10)$$

Dispersion equation has a form:

$$(P-\eta\varepsilon(\rho+1))(S-\eta(\beta_b+\rho\beta_a))-\eta^2\rho(\xi_a+\xi_b)^2 = 0. \qquad (4.11)$$

Eigen values of the problem ν must be found from the eq.(4.11), where a dependence on ν is contained in P, S, ρ, ξ. If η=0, we get E_z modes (when P=0, i.e. $p_\nu(\gamma_p b,\gamma_p a)$=0), and H_z modes (when S=0, i.e. $s_\nu(\gamma_p b,\gamma_p a)$=0). If η is not zero but small, we can solve (4.11) in the first approach, using linear approximation of Bessel functions and their derivatives near the roots of $p_\nu(\gamma_p b,\gamma_p a)$=0:

$$p_\nu(\gamma_p a,\gamma_p b) \approx p_{\nu_0}(\gamma_p a,\gamma_p b) + (\nu-\nu_0)\frac{\partial}{\partial\nu} p_\nu(\gamma_p a,\gamma_p b)\Big|_{\nu=\nu_0}, \qquad (4.12)$$

and so on.

The components of the eigen vector can be written as

$$A/D = -\frac{P-\eta\varepsilon(\rho+1)}{\eta(\xi_a+\xi_b)} = -\frac{\eta(\xi_a+\xi_b)}{S-\eta(\beta_b+\rho\beta_a)};$$

$$B = \eta(-\varepsilon A+\xi_a D);$$

$$C = \eta(-\xi_a A+\beta_a D). \qquad (4.13)$$

These eigen values and eigen vectors must be used at calculating the impedance (3.15) (in ν, E and N).

4.3. The horizontal walls of finite conductivity.

In the case of horizontal walls of finite conductivity the eq. (4.6) gives us the new value of k_{zp}:

$k_{z0}=\sqrt{-\eta_z k/g}$ - for H_z mode with p=0;

$$k_{zp}=\frac{\pi p}{2g}-\frac{\eta_z}{g}\left(\frac{2gk}{\pi p}\right)^{\pm 1} \quad \text{- for } H_z\ (E_z) \text{ modes with } p\neq 0. \qquad (4.14)$$

New values of k_{zp} determine new values of γ_p, as $\gamma_p^2+k_{zp}^2=k^2$. Thus, when we find ν, the roots of the dispersion equations for zero boundary conditions (2.6) at r=a,b, we must deal with complex arguments. The shift of the eigen value due to the finite conductivity of horizontal walls can be found in the first approach as

$$\Delta\nu=\nu-\nu_0=-(\gamma_p-\gamma_{p_0})\left.\frac{\partial f/\partial\gamma}{\partial f/\partial\nu}\right|_{\nu_0,\gamma_{p_0}}, \qquad (4.15)$$

where $f=p_\nu(\gamma_p b,\gamma_p a)$ for E_z modes and $f=s_\nu(\gamma_p b,\gamma_p a)$ for H_z modes; the index "0" denotes the values at $\eta_z=0$.

Note once more that in this case E_z and H_z modes are not coupled.

4.4. All four walls of finite conductivity (for not degenerated modes).

If we consider the case, when the shift of the eigen value due to the walls finite conductivity is much less then the distance between neighbour eigen values, i. e. when the modes E_z and H_z in the curved waveguide are practically not coupled due to the vertical walls finite conductivity, we can get the solution satisfying the Leontovich conditions on

all four walls in the first order of η (η_z).

If the modes E_z and H_z are not coupled, the roots of $p_\nu(\gamma_p b,\gamma_p a)=0$ and $s_\nu(\gamma_p b,\gamma_p a)=0$ are separated, i. e. the roots of eq. (4.11) are such that

1) $p_\nu(\gamma_p b,\gamma_p a)\sim\eta$ and $s_\nu(\gamma_p b,\gamma_p a)\sim\eta^0$, A/D $\sim\eta$; or (4.16)

2) $s_\nu(\gamma_p b,\gamma_p a)\sim\eta$ and $p_\nu(\gamma_p b,\gamma_p a)\sim\eta^0$, D/A $\sim\eta$. (4.17)

The first case is H_z mode with a small contribution of E_z, and the second - oppositewise. To take into account the finite conductivity of the horizontal walls, we can solve the eq. (4.14) and find new values of k_{zp} and γ_p for E_z and H_z modes, and then substitute the gotten k_{zp} and γ_p into (4.10) and (4.11) and chose the solution corresponding to (4.16) for H_z mode and (4.17) for E_z mode. The eigen vector can be determined as in (4.13) with the proper values of

5. APPROXIMATE EIGEN VALUES ν

In this section, we want, at first, to adduce the dispersion functions, a dependence of the longitudinal wave number ν on the frequency; then we will compare the shift of the longitudinal wave number due to the walls finite conductivity for straight and curve waveguide; and finally, we will compare the eigen modes delay due to the curvature and finite conductivity.

5.1. Dispersion equation solutions for the ideal waveguide.

The approximate eigen values of the dispersion equations are derived in App.3. Here we adduce the final approximation for small δ.

a) $\nu<x<y$.

$$p_\nu(y,x)=0 \quad \text{at } \nu_E=\nu_0+\frac{1+5\mathrm{ctg}^2\beta_0}{8\nu_0\sin\beta_0},$$

$$s_\nu(y,x)=0 \quad \text{at } \nu_H=\nu_0-\frac{3+7\mathrm{ctg}^2\beta_0}{8\nu_0\sin\beta_0}, \qquad (5.1)$$

where

$\nu_0=\left(\bar{x}^{-2}-(\pi n/\delta)^2\right)^{1/2}$, $\sin\beta_0=\pi n/\delta\bar{x}$, $\bar{x}=(x+y)/2$, $\delta=(y-x)/\bar{x}$, n is integer.

We can see that $(\nu_E-\nu_H)$ is a very small value, of order $1/x$, that means that splitting due to the curvature decreases when the frequency increases, and the eigen modes become practically the eigen modes of the straight waveguide. Thus the mode coupling due to the finite conductivity of the vertical walls can lead to the separation not on the E_z and H_z modes (as because of the curvature), but rather on E_r and H_r modes (because of the finite conductivity).

b) $x<\nu<y$.

$$p_\nu(y,x)=0 \qquad \nu_E\approx y\left(1-\xi\left(C_{1E}/y\right)^{2/3}\right),$$

$$s_\nu(y,x)=0 \qquad \nu_H\approx y\left(1-\xi\left(C_{1E}/y\right)^{2/3}\right), \qquad (5.2)$$

where $\xi = 3^{2/3}/2 \approx 1.04$; $C_{1\,E,H}=\pi(1-1/2\pm1/4)$, $l\geq1$.

c) Zero H_z mode.

$$\nu_H\approx\gamma a\left(1+\frac{\delta}{2}(1+(\delta\bar{x})^3/(30\bar{x}))\right), \text{ where } (\delta\bar{x})/(30\bar{x})^{1/3}\ll1. \qquad (5.3)$$

The distance between nearest ν_E and ν_H in this case is practically half of the distance between neighbour ν_E (or ν_H), this distance can be estimated as

$$\Delta\nu_{\text{nearest}}\approx\frac{2}{3}\xi(\gamma a/C_1)^{1/3}\Delta C_1 = \frac{\pi}{3}\xi(\gamma a/C_1)^{1/3}\approx(\gamma a/C_1)^{1/3}.$$

Thus the modes E_z and H_z are not coupled even at the finite walls conductivity (if the shift of ν due to the finite conductivity remains much less than $\Delta\nu_{\text{nearest}}$).

5.2. Dispersion equation solutions for the finite conductivity of vertical walls.

For the longitudinal wavenumber shifts estimation we can use the Bessel function approximation given in App.2. A Debye approximation is sufficient for the "waveguide" modes with $\nu<\gamma a$; for the "delayed" modes we can use the approximation (A2.4).

At first, we consider a case with finite conductivity of vertical walls.

If $|\nu-\gamma a|\gg|\gamma a-\gamma b|$, then in the eq. (4.11) we can put:

$$P\approx\mathrm{tg}(\varphi_1-\varphi_2)/\sin(\alpha);\ S\approx\mathrm{tg}(\varphi_1-\varphi_2)\sin(\alpha);\ \rho\approx1;$$

$$\beta_a\approx\beta_b;\quad \xi_a\approx\xi_b;\quad \cos\alpha_1=\nu/\gamma a;\quad \cos\alpha_2=\nu/\gamma b;\quad \cos\alpha\approx\nu/\langle r\rangle,$$

$$\langle r\rangle=(a+b)/2;\ \varphi_{1,2} = \nu(\mathrm{tg}\alpha_{1,2} - \alpha_{1,2})-\pi/4. \qquad (5.4)$$

The eq. (4.11) transforms into the equation for a straight waveguide, and it's solution can be written as

$$tg(\varphi_1-\varphi_2)=2\eta\left(\frac{k}{k_x}\right)^{\pm 1}, \text{ where } k_x=\left(\gamma^2-(\nu/\langle r\rangle)^2\right)^{1/2}. = \gamma\sin(\alpha).$$

(5.5)

The order derivatives of P and S at their zeros are (App.2)

$$\partial P/\partial\nu = \delta\cos\alpha/\sin^2\alpha, \qquad (5.6)$$

$$\partial S/\partial\nu \approx \partial P/\partial\nu \sin^2(\alpha) = \delta\cos\alpha. \qquad (5.7)$$

The shift of ν can be determined as

$$\Delta\nu = \frac{P}{\partial P/\partial\nu} = \frac{S}{\partial S/\partial\nu} = tg(\varphi_2-\varphi_1)tg(\alpha)/\delta,$$

$$\Delta\nu_E = 2\eta\frac{k}{\gamma\delta\cos(\alpha)} = \frac{2\eta k}{\nu\delta} = 2\eta(k/k_x)(k_x/\nu)/\delta,$$

$$\Delta\nu_H = 2\eta\frac{\gamma\sin^2(\alpha)}{k\delta\cos(\alpha)}. \qquad (5.8)$$

For a straight waveguide

$\sin(\alpha)=k_x/\gamma$; $\cos(\alpha)=k_y/\gamma$;

$$\Delta k_y = -\Delta k_x\, k_x/k_y = 2\eta\left(\frac{k}{k_x}\right)^{\pm 1}\frac{1}{d}tg(\alpha). \qquad (5.9)$$

Comparing (5.8) and (5.9), we see that in the limit $\nu\to 0$ the shifts of the longitudinal wavenumber for curve and straight waveguide coincide.

As for "delayed" modes, we can solve the dispersion equation assuming that the modes E_z and H_z are not coupled. In this case the eq.(4.11) separates on two equations:

$$P-\eta\varepsilon(\rho+1) = 0 \qquad \text{for } E_z \text{ modes,} \qquad (5.10)$$

$$S-\eta(\beta_b+\rho\beta_a) = 0 \qquad \text{for } H_z \text{ modes.} \qquad (5.11)$$

These equations lead to

$$\Delta\nu_E = \frac{\eta\varepsilon(\rho+1)}{\partial P/\partial\nu} \quad ; \qquad (5.12)$$

$$\Delta\nu_H = \frac{\eta(\beta_b+\rho\beta_a)}{\partial S/\partial\nu}. \qquad (5.13)$$

Approximation formulas (A2.4) give for E_z modes:

$$\rho\approx\frac{\sin\beta}{4\,sh\alpha}e^{2\psi}\gg 1 \text{ (for } \psi>1), \quad \partial P/\partial\nu \approx \rho/\cos\beta,$$

$$\Delta\nu_E = \frac{\eta\varepsilon(\rho+1)}{\partial P/\partial\nu}\approx \eta\varepsilon\cos\beta \approx \eta\varepsilon. \qquad (5.14)$$

As for H_z modes, we have:

$$\rho\approx 4\frac{\sin\beta}{sh\alpha}e^{-2\psi}\ll 1 \text{ (for } \psi>1), \quad \partial S/\partial\nu \approx \sin^2\beta/\cos\beta,$$

$$\Delta\nu_H = \frac{\eta(\beta_b+\rho\beta_a)}{\partial S/\partial\nu}\approx \frac{\eta\beta_a\cos\beta}{\sin^2\beta} \approx \frac{\eta\beta_a}{\sin^2\beta}. \qquad (5.15)$$

Note that both for delayed modes and for "waveguide" ones the shift of H_z modes is much more than of E_z modes.

5.3. Dispersion equation solutions for the finite conductivity of horizontal walls.

In the case of finite conductivity of horizontal walls, the dispersion equation solution is

$$\Delta\nu_E=-\Delta\gamma_E\frac{\partial p_\nu(\gamma b,\gamma a)/\partial\gamma}{\partial p_\nu(\gamma b,\gamma a)/\partial\nu}=-\eta_z\left(\frac{k}{k_z}\right)\frac{k_z}{\gamma g}\frac{\partial p_\nu(\gamma b,\gamma a)/\partial\gamma}{\partial p_\nu(\gamma b,\gamma a)/\partial\nu};$$

$$\Delta\nu_H=-\Delta\gamma_H\frac{\partial s_\nu(\gamma b,\gamma a)/\partial\gamma}{\partial s_\nu(\gamma b,\gamma a)/\partial\nu}=-\eta_z\left(\frac{k_z}{k}\right)\frac{k_z}{\gamma g}\frac{\partial s_\nu(\gamma b,\gamma a)/\partial\gamma}{\partial s_\nu(\gamma b,\gamma a)/\partial\nu}. \qquad (5.16)$$

At the assumptions of App.2 (for the formula A2.6 and further), for the "waveguide" modes with $\nu<\gamma a$ and for "delayed" modes with $\gamma a<\nu<\gamma b$, the result are similar to the straight waveguide ones:

$$\Delta\nu_E=-\Delta\gamma_E\frac{r_\nu a+q_\nu b}{-(r_\nu a+q_\nu b)\gamma/\nu}=\Delta\gamma_E\nu/\gamma=\eta_z\left(\frac{k}{k_z}\right)\frac{k_z}{\gamma g}\nu/\gamma; \qquad (5.17)$$

$$\Delta\nu_H=-\Delta\gamma_H\frac{a\,\partial s_\nu/\partial(\gamma a)+b\,\partial s_\nu/\partial(\gamma b)}{-(a\,\partial s_\nu/\partial(\gamma a)+b\,\partial s_\nu/\partial(\gamma b))\gamma/\nu}=$$

$$=\Delta\gamma_H\nu/\gamma=\eta_z\left(\frac{k_z}{k}\right)\frac{k_z}{\gamma g}\nu/\gamma. \qquad (5.18)$$

For the straight waveguide

$$\Delta k_y=-\Delta k_z k_z/k_y=\eta_z\left(\frac{k}{k_y}\right)\frac{1}{g} \qquad (E_z \text{ modes}); \qquad (5.19)$$

$$\Delta k_y=\eta_z\left(\frac{k_z}{k}\right)\frac{k_z}{k_y g} \qquad (H_z \text{ modes}). \qquad (5.20)$$

Note that in the case of finite conductivity of horizontal walls, the shift of E_z modes is much more than of H_z modes.

Our analysis shows that the vertical walls with finite

conductivity damp mainly H_z modes (i. e. E_x or E_r modes in the case of modes coupling), and the horizontal walls with finite conductivity damp E_z modes. In reality both four walls have finite conductivity, and all modes damp, due to horizontal or vertical walls. A reasonable method to describe simultaneously damping due all four walls for the uncoupled modes was discussed in the section 4. For estimations, we can sum the shifts if the longitudinal wavenumber due to both couples of walls.

The parameters of the resonances are estimated in App.4. The resulting estimations for the resonant frequencies, bands and shunt resistances for a beam placed in the center of the chamber at R=(a+b)/2, for modes with $p\neq0$, $l\neq0$, are given in section 9.

5.4. Comparison of resonant frequencies for straight and curve waveguide.

The modes of a straight waveguide are also somewhat delayed due to the finite conductivity of chamber walls. It is interest to see, if in the straight waveguide the resonances can appear due resistive delaying, and compare them with the curve waveguide resonances. To avoid repeating, we will consider only the case of finite conductivity of vertical walls; the results for vertical walls are the same with replacement of the indexes $x\to z$ and $z\to x$.

The resonant factor for a straight waveguide has a form (see (3.18)):

$$\frac{2k_y}{(k/\beta)^2-k_y^2}=\frac{2k_y}{k_x^2+k_z^2+k^2/(\gamma^2-1)}, \qquad (5.21)$$

where transverse components of the wave vector k_x, k_y have a complex addition due to the finite conductivity. If the dispersion equations (4.5) or (4.6) have the solution, which

turns the real part of the resonant factor denominator into zero at some frequency, then we have a resonance at this frequency. At $\beta=1$ (for simplicity) and $\eta=0$:

$$k^2-k_{y0}^2=(k_{x0}^2+k_{z0}^2)=k_{\perp 0}^2;$$

A resonance appears if

$$\mathrm{Re}(k^2-k_y^2)=\mathrm{Re}(k_\perp^2)=0. \qquad (5.22)$$

The solution of equations (4.5) and (4.6) in the approach $\Delta k_x d \ll 1$ gives a result not consisting with this approach, thus, the equations require more accurate solution.

Separating eq.(4.5) for H_x modes on real and imaginary parts, we get a system three equations (together with the resonant condition (5.22)):

$$\begin{cases} \left|\dfrac{\mathrm{th}(Y)}{\cos(X)/\mathrm{ch}(Y)+1}\dfrac{(X+Y)}{X-Y}\right| = \alpha_H, \\ \sin(X) = \dfrac{X-Y}{X+Y}\,\mathrm{sh}(Y) \\ Y^2=X^2+4a^2\ , \end{cases} \qquad (5.23)$$

where

$Z=k_x d=X+iY$, $a=k_z d/2$ (real), $\eta_0=(R\sigma Z_0)^{-1/2}$,

$\delta=d/R$, $\alpha_H=(kR)^{-1/2}\delta\eta_0$.

For E_x modes the system slightly differs:

$$\begin{cases} \left|\dfrac{\mathrm{th}(Y)}{(\cos(X)/\mathrm{ch}(Y)+1)}\dfrac{(X^2+Y^2)}{(X-Y)}\right| = \alpha_E, \\ \sin(X) = \dfrac{X+Y}{X-Y}\,\mathrm{sh}(Y), \\ Y^2=X^2+4a^2\ , \end{cases} \qquad (5.24)$$

$$\alpha_E=(k^3d^2/\sigma Z_0)^{-1/2}=(kR)^{3/2}\delta,$$

but the difference is not essential.

Substituting $Y=\pm(X^2+4a^2)^{1/2}$ into the second equation of (5.23), we get one independent equation for X, which can be solved by iterations, with the zero approach $X_0=k\pi$. The number of resonant modes is determined by l_{max} ($X_{max}=l_{max}\pi$), at which this equation still has the real root. This number can be estimated via the condition

$$|\mathrm{sh}(Y)(X-Y)/(X+Y)| \sim 1.$$

For $X, Y \gg 2a$ and $Y \gg 1$ it gives $l_{max} \approx \ln(a^2/2)/\pi$.

The resonant frequencies for $0 < l < l_{max}$, $Y \gg 1$, $2a \ll X$ can be estimated as

$$(kR)_{res}=(\eta_0/\delta)^2(l\pi+\sqrt{(l\pi)^2+4a^2}\ )^2\approx(\eta_0/\delta)^2(2l\pi)^2 \text{ for } H_x \text{ modes},$$

$$(kR)_{res}=1/(\delta\eta_0)^{2/3}\,((2(l\pi)^2+4a^2)/((l\pi+\sqrt{(l\pi)^2+4a^2}\ ))^{2/3}\approx$$

$$\approx (l\pi/\delta\eta_0)^{2/3} \text{ for } E_x \text{ modes.} \qquad (5.25)$$

One can see that if the walls conductivity increases, resonant frequencies of H_x modes tend to zero, and can not have any comparison with the resonances in the curve

waveguide. The resonant frequencies of E_x modes, however, tend to infinity with increasing the walls conductivity, therefore, we can compare the effects of curvature and finite conductivity for these modes.

The estimation expressions (5.25) were gotten under assumptions corresponding to the following expressions for resonant frequencies (App.4):

$$p\neq 0,\ l\neq 0 \quad A\gg 1 \Rightarrow (kb)^2=x^3+(k_z b)^2=(3C_l)^2/(2\delta_r)^3+(\pi p/2\delta_z)^2$$

$$A\gg 1 \Rightarrow (kb)\approx(3C_l)/(2\delta_r)^{3/2}. \qquad (5.26)$$

Comparing (5.25) and (5.26), we can see that the resistive resonance in the straight waveguide appears at the same frequency as in the curve waveguide with the same cross section, if

$$\sigma \approx (l\pi/dZ_0)/\delta^{3/2}.$$

Taking parameters of Berkley storage ring (see next section), we find that

1) for equal radial camera dimension d and given curvature of Berkley storage ring the resonant frequency of the straight waveguide first resonance (l=1) due to the finite conductity will be equal to the resonant frequency due to the curvature in the storage ring, if $\sigma\approx 2.5\cdot 10^3\,\Omega^{-1}m^{-1}$, four orders less than the copper conductivity;

2)for given conductivity $\sigma\approx 3.54\cdot 10^7\,\Omega^{-1}\,m^{-1}$ the resonant frequencies of straight and curve waveguides are equal, if the storage ring curvature is $\delta\approx 3\cdot 10^{-6}$, about three orders less than the Berkley storage ring curvature.

The parameters at which the resonances due to the finite conductivity in the straight waveguide and due to the curvature in the toroidal waveguide appear at equal frequencies are far behind the region of parameters to be considered (section 6, tab.1). Moreover, the resistive

resonances in the straight waveguide appear at such strong damping, that all the consideration, when we dropped the higher order terms in spreading all functions over powers of η, becomes not correct. Therefore, we can say that for the parameters under consideration the resonances only due to the finite conductivity do not appear.

6. THE RESULTS OF CALCULATIONS

6.1. The computation code.

A code was written calculating the impedance at the formula (3.16), summing up a given number of terms for next problems:

1. a finite conductivity of vertical walls;
2. a finite conductivity of horizontal walls;
3. a finite conductivity of all four walls (summing up only "delayed", uncoupled modes).

The impedance can be scanned over the frequency (i. e. over the harmonic number) and over the transverse beam position (r and z). In the case of finite conductivity of one couple walls a difference of the impedances for the curve and straight waveguide; in the case of the finite conductivity of all four walls only the impedance of the curve waveguide is calculated, the results are reliable in the resonant regions.

6.2. The parameters of the considered storage rings.

The calculations were made for Berkley storage ring (to compare the results with [1]) and for the project of the Novosibirsk phi-factory as an example of a rather non-circular machine with big curvature.

In the table 1, the necessary parameters of considered accelerators are given:

Tab.1

Parameters	Berkley storage ring	Novosibirsk phi-factory
Radius of the ring $R_{ring} = l_{ring}/2\pi$	30 m	32.87 m
Vertical camera dimention $2\delta_z = h/R_{ring}$	$0.833\cdot10^{-3}$	$0.122\cdot10^{-2}$
Horizontal camera dimention $\delta = d / R_{ring}$	$1.667\cdot10^{-3}$	$0.122\cdot10^{-2}$
Bending magnets radius R_{mag} / R_{ring}	1	0.0085
Bending magnets length $l_{mag} / 2\pi R_{mag}$	1	1.5
Beam vert. dimention Δ_z / h	0.1	0.1
Camera walls conductivity σ	$3.54\cdot10^{7}\ \Omega^{-1}m^{-1}$	
Curvature d / R_{mag}	$1.667\cdot10^{-3}$	0.15

6.3. The comparison of results of calculations for Berkley storage ring with results of Warnock [1].

Consider at first the Berkley storage ring, the case of vertical walls with finite conductivity.

The fig.3 shows r- and z-dependence of the real part of the impedance at the frequency $f=2\cdot10^{4}\cdot f_0$, lower than the first resonance $f\approx1\cdot10^{5}\cdot f_0$. Fig.3a and 3b represent the impedances of the straight and curve waveguides; fig.3c and

3d represent the difference of the impedances of the straight and curve waveguide. A number of summed modes is 10×10. The calculations show that increasing the number of summed modes does not contribute essentially into the difference of the impedances of the curve and straight waveguide.

It is obvious that the contribution to the impedance due to the curvature, at scanning in z-direction, is symmetrical relatively z=o. But if you scan in r-direction, the curvature contribution is positive near the outer wall and negative at the inner wall of a toroidal chamber.

Fig.4 shows the same pictures in the case of the horizontal walls finite conductivity. Note that the curvature contribution has the opposite sign in comparison with the case of the vertical walls with finite conductivity. The reason is the next. In the case of horizontal walls with finite conductivity the eigen modes split on E_z and H_z modes, the main contribution to the impedance gives E_z mode with the longitudinal field described by a function p_ν, representing a sine with increasing in the positive r-direction amplitude. In the case of vertical walls with finite conductivity the eigen modes split on E_x and H_x modes, the main contribution to the impedance gives H_x mode with the longitudinal field described by a function s_ν, representing a sine with decreasing in the positive r-direction amplitude. It leads to the different sign of the eigen modes contribution to the resistive impedance in these two cases.

In the resonant region the picture changes. The radial dependence of the curvature contribution to the resistive impedance at the more high frequency ($f=2\cdot10^{5}\cdot f_0$) is shown in fig.5 for the cases of vertical (a) and horizontal (b) walls with finite conductivity. We can see that the narrow and wide resonances exchange their positions in these two

cases. The estimation formulas for Δr - radial widths of resonances agree with numerical calculations. Thus, for the first resonance (H_z mode with p=1,l=0) placed at r = a+0.754(b-a), the numerical calculations give the same radial width of the resonance as the estimation:

$\Delta r/d = 3.2 \cdot 10^{-3}$.

If r-dimension of the beam is of the same order as the radial width of the resonance or more, we must average the obtained impedance over the beam cross section (it will be made in the next section).

Finally, we adduce the frequency dependence of the impedance (fig.6) co compare our results with [1]. They appear to be in good agreement. It confirms that our waveguide consideration is admissible. As this paper, as [1], is mainly turned to the problem of the resonances, we must emphasize that in the resonant regions the impedance is described by the only term of the series (3.15), with the resonant factor having a very simple form (see above). That is why we propose our work.

6.4. The results of calculations for a non-circular storage ring with big curvature.

As an example of the machine with big curvature we consider a project of the Novosibirsk phi-factory (a curvature of the bent segments is ~ 100 times more than the curvature of the Berkley storage ring, see tab.1). A cross section of the machine is round with a diameter d given in tab.1; for our estimations, we consider a square cross section of the same dimension.

For the phi-factory, the bending magnets' radius R_{mag} and length l_{mag} differ essentially from the radius R_{ring} and perimeter $l_{ring}=2\pi R_{ring}$ of the machine, that's why the impedance at the n-th harmonic of the revolution frequency

$\omega=n\omega_0$ must be calculated by the formula (3.15) for the same frequency ω and the ring of the radius R_{mag}, i. e. instead of the revolution frequency ω_0 we must substitute $\omega_0'=\omega_0(l_{ring}/2\pi R_{mag})$; the beam radial position R must be taken also relatively the ring of the radius R_{mag}. The result must be multiplied by $l_{mag}/2\pi R_{mag}$ (as in (3.15) the impedance was calculated per one turn, and now we must take into account the real angular length of the magnets.

Fig.7 represents frequency dependence of the impedance of the camera with all four walls with finite conductivity (taking into account only resonant terms). The resonances appear at the harmonic numbers approximately ten times less than in Berkley storage ring.

Fig.8 represents a radial dependence of the impedance in the resonant region (at frequency $f=1\cdot10^4\cdot f_0$ and $f=2.5\cdot10^4\cdot f_0$). These calculations were made for a beam with delta-function radial density distribution. The radial width of the resonances is here $\Delta r/d\sim10^{-4}$, the peak value of the impedance

$$\mathrm{Re}(Z/n)_{max}\sim200\ \mathrm{Ohm}.$$

The tab.2 contains parameters of some first resonances for two considered storage rings (modes number, resonant harmonic number, a width of a resonance in n and r variables and shunt resistance).

We can see that the resonant frequencies and the shunt impedances for Berkley storage ring are in good agreement with the simulations of Warnock [1].

Comparing the radial width of the resonances with the phy-factory beam radial dimension σ_r= 0.5mm, or $\sigma_r/d=0.012$, we see that the resonances are much narrower than the real beam radial dimension. Therefore, the impedance must be averaged over the beam cross section. For a rough estimation

Tab. 2

p nE,H	n, 10^4	f, GHz	Δn/n	Δr/d, 10^{-3}	R_s/n, Ohm
		Berkley storage ring:			
1 0(H)	11.89	189.33	1000	2.96	2.52
1 1(E)	17.22	274.20	2500	3.9	1.25
1 1(H)	22.59	359.71	1000	1.02	4.84
1 2(E)	28.45	453.03	4500	3.03	0.59
1 2(H)	34.69	552.39	1300	0.75	3.1
1 3(E)	40.94	651.91	5500	2.53	2.49
		Phy-factory:			
1 0(H)	1.108	16.103	4.5(220)	0.126	212.5(6.57)
1 1(E)	2.032	29.531	10.8(660)	0.112	28.2(0.805)
3 0(H)	2.668	38.775	9.6(440)	0.145	1.73(0.063)
1 1(H)	2.972	43.193	7.2(1060)	0.045	72.2(0.82)
3 1(E)	3.498	50.837	10.4(760)	0.087	4.2(0.095)
1 2(E)	4.023	58.467	17.9(1480)	0.079	4.34(0.091)
3 1(H)	4.272	62.086	8.2(1080)	0.049	10.58(0.24)

of the shunt impedance we must multiply it on a factor $\chi \sim \Delta r/\sigma_r$, when $\chi<1$; when $\chi>1$, we can retain the shunt impedance for a beam with the zero width. In the next section we will adduce more accurate account of the beam radial dimension. The resonant parameters with the account of the finite radial dimension of the beam are given in the table 2 in the brackets.

7. FINITE RADIAL DIMENSION OF A BEAM

Return to the expression for the impedance (3.15):

$$Z_1(\omega) = -2\pi R^2 \sum_s \frac{\Lambda_p}{iN_s} \frac{2\nu}{(\omega/\omega_o)^2-\nu^2} E^2_{s,q}(R) \sin^2(k_{zp} z_0 + \pi p/2),$$

$\omega_0 = \beta c/R$.

The radial dependence of the impedance contains the resonant factor $2\nu/((\omega/\omega_o)^2-\nu^2)$ and the modes factor $(RE_{s,\theta}(R))^2$. The character dimension of the field changing is d/m (m is the radial number of the mode), it retains much more than the beam radial dimension for a great number of first resonant modes. Thus, averaging the impedance over the beam cross section, we can average only the resonant factor, supposing the slowly changing modes factor to be constant.

For a simplicity, we suppose the radial density distribution to be constant in the beam cross section:

$$\rho(R) = \begin{cases} 1/\sigma_r, & |R-R_0| < \sigma_r/2, \\ 0, & |R-R_0| > \sigma_r/2. \end{cases} \qquad (7.1)$$

Averaging the resonant factor, we get (denoting $x_0 = \omega R_0/\beta c$, $\Delta = \omega\sigma_r/\beta c$):

$$\langle 2\nu/((\omega/\omega_o)^2-\nu^2) \rangle = \int 2\nu/((\omega/\omega_o(R))^2-\nu^2)\rho(R)dR =$$

$$= \frac{1}{\Delta}\int_{-\Delta/2}^{\Delta/2}\left(\frac{1}{x+x_0-\nu} - \frac{1}{x+x_0+\nu}\right)dx \approx -\frac{1}{x_0+\nu} + \frac{1}{\Delta}\int_{-\Delta/2}^{\Delta/2}\frac{dx}{x-(\nu-x_0)} =$$

$$= -\frac{1}{x_0+\nu} + \frac{1}{2\Delta}\ln\left(\frac{(\Delta/2-(\nu_r-x_0))^2+\nu_i^2}{(\Delta/2+(\nu_r-x_0))^2+\nu_i^2}\right) + \frac{i}{\Delta}\operatorname{arctg}\frac{x-(\nu_r-x_0)}{\nu_i}\Bigg|_{-\Delta/2}^{\Delta/2}. \qquad (7.2)$$

At $\nu_r = x_0$ (omitting the first term, negligibly small near the resonance):

$$\langle 2\nu/((\omega/\omega_o)^2-\nu^2) \rangle = 2i/\Delta \operatorname{arctg}(\Delta/\nu_1). \qquad (7.3)$$

In the limit $\Delta \to 0$

$$<2\nu/((\omega/\omega_o)^2-\nu^2)> = 2i/\nu_i; \qquad (7.4)$$

But in the contrary case, if $\Delta \gg \nu_i$, the resonant peak is

$$<2\nu/((\omega/\omega_o)^2-\nu^2)> = \pi i/\Delta, \qquad (7.5)$$

the resonance peak is $\pi\nu_i/2\Delta$ less than in the case of zero beam width.

This result agrees with the rough estimation given in the previous section.

Finally, we note, that if the resonant bent is more than the beam radial dimension ($\nu_i \geq \Delta$) or if the resonant peak is remote ($\Delta \leq |\nu - x_0|$) , then averaging is not necessary:

$$<2\nu/((\omega/\omega_o)^2-\nu^2)> = -\frac{1}{x_0+\nu} + \frac{1}{\Delta}\ln\left|\frac{1-\Delta/(2(\nu-x_0))}{1+\Delta/(2(\nu-x_0))}\right| \approx$$

$$\approx -\frac{1}{x_0+\nu} - \frac{1}{\Delta}\frac{\Delta}{\nu-x_0} = \frac{2\nu}{x_0^2-\nu^2} = 2\nu/((\omega/\omega_o(R_0))^2-\nu^2). \qquad (7.6)$$

Fig.9. shows one of the first resonant peaks for different radial beam dimensions. The shunt impedance dependence on the radial beam dimension is given in a fig.10. We can see that for the parameters of the phi-factory the shunt impedance of the considered resonance is 4.5 Ohm instead of 155.4 Ohm for a beam with zero radial beam dimension.

Fig.11 represents a frequency dependence of the impedance of the phi-factory, for the nonzero radial beam dimension and all four camera walls with finite conductivity. The peak impedances are approximately 30-100 times less than given in a fig.8 for a beam with zero radial beam dimension.

8. ESTIMATION FORMULAS FOR RESONANT PARAMETERS

The parameters of the resonances are estimated in App.4. The resulting estimations for the resonant frequencies, bands and shunt resistances for a beam placed in the center of the chamber at R=(a+b)/2, for modes with $p \neq 0$, $l \neq 0$, are given in section 9.

$$A = \left(6\beta\delta_z C_l/\pi p\delta\right)^{2/3} \gg 1.$$

Denotations:

$\delta=(b-a)/a$; $\delta_z=g/R$; $\nu_i=\mathrm{Im}(\nu)$;

$\nu_i=\mathrm{Im}(\eta)k/(\gamma\delta_z)\approx\sqrt{k/\sigma Z_0}/\delta_z$ (E_z modes),

$\nu_i=\mathrm{Im}(\eta)\gamma/(k\beta^2)\approx\sqrt{k/\sigma Z_0}/\delta$ (H_z modes);

$C_l=\pi(l\mp 1/4)$ for E_z, H_z modes ($l \geq 1$).

1)The resonant frequencies:

$$(kb)^2=(3C_l)^2/\delta^3+(\pi p/2\delta_z)^2\approx(3C_l)^2/\delta^3$$

2)The resonant bands:

$$\Delta(n)=\left|2\nu_i\frac{(3C_l)^2/\delta^3}{(\pi p/2\delta_z)^2}\right|$$

3)The resonant band in r-direction:

$$\Delta r/(b-a)\approx \nu_i/(kb\delta)$$

4)The resonant peaks: $R_{shunt}=Re(Z(\omega)/n)_{max}$

$$R_{shunt} \approx \frac{\pi^2 Z_0 p}{(kb)^2 \nu_i \delta_z^2 \delta^{1/2}} \qquad \text{(for } E_z, H_z \text{ modes)}$$

or

4)The resonant peaks: $R_{shunt}=Re(Z(\omega)/n)_{max}$

$$R_{shunt} \approx \frac{\pi^2 Z_0 p}{(kb)^2 \nu_i \delta_z^2 \delta^{1/2}} \qquad \text{(for } E_z, H_z \text{ modes)}$$

or

$$R_{shunt} \approx \frac{\pi^2 Z_0 \sqrt{2b\sigma Z_0}\, p}{(kb)^{5/2} \delta_z \delta^{1/2}} \qquad (E_z \text{ modes}),$$

$$R_{shunt} \approx \frac{\pi^2 Z_0 \sqrt{2b\sigma Z_0}\, \delta^{1/2} p}{(kb)^{5/2} \delta_z^2} \qquad (H_z \text{ modes}).$$

For more accurate estimations see App.4.

Appendix 1

INTEGRALS OF BESSEL FUNCTIONS CROSS-PRODUCTS

$$\nu\int_a^b p_\nu^2(\gamma r,\gamma a)\frac{dr}{r} = \frac{\gamma b}{2}\left(p_\nu\, \partial r_\nu/\partial\nu - r_\nu\, \partial p_\nu/\partial\nu\right)\Big|_{(\gamma b,\gamma a)} \qquad \text{(A1.1)}$$

$$\nu\int_a^b q_\nu^2(\gamma r,\gamma a)\frac{dr}{r} = \frac{\gamma b}{2}\left(q_\nu\, \partial s_\nu/\partial\nu - s_\nu\, \partial q_\nu/\partial\nu\right)\Big|_{(\gamma b,\gamma a)} \qquad \text{(A1.2)}$$

$$\nu\int_a^b p_\nu(\gamma r,\gamma a)q_\nu(\gamma r,\gamma a)\frac{dr}{r} = \frac{\gamma b}{2}\left(p_\nu\, \partial s_\nu/\partial\nu - r_\nu\, \partial q_\nu/\partial\nu\right)\Big|_{(\gamma b,\gamma a)} =$$

$$= \frac{\gamma b}{2}\left(q_\nu\, \partial r_\nu/\partial\nu - s_\nu\, \partial p_\nu/\partial\nu\right)\Big|_{(\gamma b,\gamma a)} \qquad \text{(A1.3)}$$

Appendix 2

APPROXIMATION OF BESSEL FUNCTIONS OF HIGH ORDER AND THEIR DERIVATIVES

In this section we would like to adduce the approximation formulas, which we have used at our estimations and calculations of the impedance.

1.We have chosen for the impedance calculations a Langer uniform approximation [5] for Bessel functions of high order:

$$J_\nu(x) = A(w,\nu)\ Ai(y(\nu,w)),\quad Y_\nu(x) = A(w,\nu)\ Bi(y(\nu,w)), \qquad \text{(A2.1)}$$

$x < \nu$:

$$w = \sqrt{1-(x/\nu)^2}\ ,\ y = \left(\frac{3}{2}\,\nu\,(\mathrm{arth}(w) - w)\right)^{2/3},$$

$$A(w,\nu)=\left(\frac{2}{\nu}\right)^{1/3}\left(\frac{\mathrm{arth}(w)-w}{w^3/3}\right)^{1/6}.$$

$x > \nu$:

$$w = \sqrt{(x/\nu)^2-1}\ ,\ y = -\left(\frac{3}{2}\,\nu\,(w - \mathrm{arctg}(w))\right)^{2/3},$$

$$A(w,\nu)=\left(\frac{2}{\nu}\right)^{1/3}\left(\frac{w-\mathrm{arctg}(w)}{w^3/3}\right)^{1/6}.$$

The order and argument derivatives can be easy found as

$$\frac{\partial}{\partial x} = \frac{\partial w}{\partial x}\,\frac{\partial}{\partial w}\ ;$$

$$\frac{\partial}{\partial \nu} = \frac{\partial w}{\partial \nu}\,\frac{\partial}{\partial w} + \frac{\partial}{\partial \nu} = \frac{\partial}{\partial \nu} + \left(\frac{\partial w}{\partial \nu}\,\frac{\partial x}{\partial w}\right)\frac{\partial}{\partial x} = \frac{\partial}{\partial \nu} + \left(-\frac{x}{\nu}\right)\frac{\partial}{\partial x}. \quad \text{(A2.2)}$$

2. For estimation of the dispersion equations solutions we can use the main term of the Debye asymptotic expansion ([4], 9.3.(7-22),

$$\begin{Bmatrix} J \\ Y \end{Bmatrix}_\nu (\nu/\cos\beta) = \sqrt{2/(\pi\nu\,\mathrm{tg}\beta)}\ \begin{Bmatrix} \cos(\varphi)+u(i\mathrm{ctg}(\beta))/\nu\ \sin(\varphi) \\ \sin(\varphi)-u(i\mathrm{ctg}(\beta))/\nu\ \cos(\varphi) \end{Bmatrix},$$

$$\begin{Bmatrix} J \\ Y \end{Bmatrix}_\nu' (\nu/\cos\beta) = \sqrt{\sin 2\beta/(\pi\nu)}\ \begin{Bmatrix} -\sin(\varphi)-v(i\mathrm{ctg}(\beta))/\nu\ \cos(\varphi) \\ \cos(\varphi)-v(i\mathrm{ctg}(\beta))/\nu\ \sin(\varphi) \end{Bmatrix},$$

$\varphi = \nu(\mathrm{tg}\beta - \beta)-\pi/4$;

$$\begin{Bmatrix} J \\ Y \end{Bmatrix}_\nu (\nu/\mathrm{ch}\alpha) = \sqrt{2/(\pi\nu\,\mathrm{th}\alpha)}\ \begin{Bmatrix} 1/2 \\ -1 \end{Bmatrix} e^{\pm\psi}(1\pm u(\mathrm{cth}(\alpha))/\nu),$$

$$\begin{Bmatrix} J \\ Y \end{Bmatrix}_\nu' (\nu/\mathrm{ch}\alpha) = \sqrt{\mathrm{sh}2\alpha/(\pi\nu)}\ \begin{Bmatrix} 1/2 \\ 1 \end{Bmatrix} e^{\pm\psi}(1\pm v(\mathrm{cth}(\alpha))/\nu),$$

$\psi = \nu(\mathrm{th}\alpha-\alpha)$;

$u(t)=-i(3t-5t^3)/24$, $v(t)=i(-9t+7t^3)/24$. (A2.3)

or the asymptotic formulas for in the transition region ([4], 9.3.23-9.3.28):

$$\begin{Bmatrix} J \\ Y \end{Bmatrix}_\nu (\nu + z\,\nu^{1/3}) = \pm\left(\frac{2}{\nu}\right)^{1/3}\begin{Bmatrix} Ai \\ Bi \end{Bmatrix}(-2^{1/3}z),$$

$$\begin{Bmatrix} J \\ Y \end{Bmatrix}_\nu' (\nu + z\,\nu^{1/3}) = \mp\left(\frac{2}{\nu}\right)^{2/3}\begin{Bmatrix} Ai' \\ Bi' \end{Bmatrix}(-2^{1/3}z). \quad \text{(A2.4)}$$

Finally, we want to adduce here the approximate formulas for the order-derivatives for the Bessel-functions cross-products p_ν and s_ν. In the first approach it is sufficient to derive only the Airy functions in (5.1), not taking into account the slow dependence on ν and x of the amplitude $A(\nu,w)$:

$$p_\nu(x_1,x_2)=A_1A_2(Ai(y_1)Bi(y_2)-Ai(y_2)Bi(y_1));$$

$$\frac{\partial p_\nu}{\partial \nu} \approx A_1A_2\left\{(Ai'(y_1)Bi(y_2)-Ai(y_2)Bi'(y_1))\,\frac{dy_1}{d\nu}+\right.$$

$$\left.+(Ai(y_1)Bi'(y_2)-Ai'(y_2)Bi(y_1))\,\frac{dy_2}{d\nu}\right\} \approx$$

$$\approx \frac{\partial p_\nu}{\partial x_1}\left(\frac{dy_1}{d\nu}\,\frac{\partial x_1}{\partial y_1}\right) + \frac{\partial p_\nu}{\partial x_2}\left(\frac{dy_2}{d\nu}\,\frac{\partial x_2}{\partial y_2}\right). \quad \text{(A2.5)}$$

Analogously, for $s_\nu(x_1,x_2)$ (using the Bessel equation):

$$\frac{\partial s_\nu}{\partial \nu} = \frac{\partial s_\nu}{\partial x_1}\left(\frac{dy_1}{d\nu}\frac{\partial x_1}{\partial y_1}\right) + \frac{\partial s_\nu}{\partial x_2}\left(\frac{dy_2}{d\nu}\frac{\partial x_2}{\partial y_2}\right) =$$

$$= -\left\{\left(\frac{dy_1}{d\nu}\frac{\partial x_1}{\partial y_1}\right)\left(\frac{1}{x_1}s_\nu + \left(1-(\nu/x_1)^2\right)q_\nu\right) + \right.$$

$$\left. + \left(\frac{dy_2}{d\nu}\frac{\partial x_2}{\partial y_2}\right)\left(\frac{1}{x_2}s_\nu + \left(1-(\nu/x_2)^2\right)r_\nu\right)\right\},$$

or, for $s_\nu(x_1,x_2)=0$, we have:

$$\frac{\partial s_\nu}{\partial \nu} = -\left\{\left(\frac{dy_1}{d\nu}\frac{\partial x_1}{\partial y_1}\right)\left(1-(\nu/x_1)^2\right)q_\nu + \left(\frac{dy_2}{d\nu}\frac{\partial x_2}{\partial y_2}\right)\left(1-(\nu/x_2)^2\right)r_\nu\right\}. \quad (A2.6)$$

Deriving the arguments of Airy-functions, we get:

$$\left(\frac{dy}{d\nu}\frac{\partial x}{\partial y}\right) = \begin{cases} -\frac{x}{\nu}\frac{\mathrm{arctgw}}{w} = -\frac{\beta}{\sin\beta} & (\beta = \mathrm{arctgw},\ x>\nu), \\ -\frac{x}{\nu}\frac{\mathrm{arthw}}{w} = -\frac{\alpha}{\mathrm{sh}\alpha} & (\alpha = \mathrm{arthw},\ x<\nu) \end{cases} \quad (A2.7)$$

Now, we can adduce the approximate values of the order derivatives at $p_\nu(x_1,x_2)=0$ or $s_\nu(x_1,x_2)=0$ for two cases:

1) $\nu<x_1<x_2$; let $|w_1-w_2| \ll w_1$

$$\frac{\partial p_\nu}{\partial \nu} \approx r\frac{\beta_1}{\nu\sin\beta_1} + q\frac{\beta_2}{\nu\sin\beta_2}; \quad (A2.8)$$

$$\frac{\partial s_\nu}{\partial \nu} = \frac{\beta_1}{\sin\beta_1}\sin^2\beta_1 q_\nu + \frac{\beta_2}{\sin\beta_2}\sin^2\beta_2 r_\nu = \beta_1\sin\beta_1 q_\nu + \beta_2\sin\beta_2 r_\nu. \quad (A2.9)$$

$$\frac{\partial p_\nu(x_1,x_2)}{\partial \nu} \approx \frac{2\cos(\varphi_1-\varphi_2)}{\pi\nu\sqrt{\mathrm{tg}\beta_1\mathrm{tg}\beta}}(\beta_2-\beta_1) \approx \frac{2\cos(\varphi_1-\varphi_2)}{\pi\nu\mathrm{tg}\beta_1^2}\delta \quad \text{(for } E_z \text{ modes)} \quad (A2.10)$$

$$\frac{\partial s_\nu(x_1,x_2)}{\partial \nu} \approx \frac{2\cos(\varphi_1-\varphi_2)}{\pi\nu\mathrm{tg}\beta_1^2}\delta\sin\beta_1\sin\beta_2. \text{(for } H_z \text{ modes)} \quad (A2.11)$$

$(\varphi_{1,2} = \nu(\mathrm{tg}\beta_{1,2} - \beta_{1,2}),\ \varphi_1-\varphi_2=\pi n)$

2) $x_1<\nu<x_2$:

For $w \ll 1$ $\left(\frac{dy}{d\nu}\frac{\partial x}{\partial y}\right) \approx -\frac{x}{\nu}$, hence

$$\frac{\partial p_\nu(x_1,x_2)}{\partial \nu} \approx -\left(r_\nu\frac{x_1}{\nu} + q_\nu\frac{x_2}{\nu}\right). \quad (A2.12)$$

$$\frac{\partial s_\nu(x_1,x_2)}{\partial \nu} = \frac{x_1}{\nu}\left(1-(\nu/x_1)^2\right)q_\nu + \frac{x_2}{\nu}\left(1-(\nu/x_2)^2\right)r_\nu. \quad (A2.13)$$

Denoting $\rho(x_1,x_2)=-r_\nu(x_1,x_2)/q_\nu(x_1,x_2)$, $\psi = \nu(\mathrm{th}\alpha-\alpha)$, we can write for $\psi>1$:

E_z modes:

$$\rho(x_1,x_2) \approx 4\frac{\mathrm{sh}\alpha}{\sin\beta}e^{-2\psi} \ll 1$$

$$\frac{\partial p_\nu(x_1,x_2)}{\partial \nu} \approx -q_\nu(x_1,x_2)\left(-\rho(x_1,x_2)\frac{x_1}{\nu}+\frac{x_2}{\nu}\right) \approx -q(x_1,x_2)_\nu/\cos\beta \quad (A2.14)$$

H_z modes:

$$\rho(x_1,x_2) \approx \frac{sh\alpha}{4sin\beta} e^{2\psi} \gg 1$$

$$\frac{\partial s_\nu(x_1,x_2)}{\partial \nu} = -q_\nu(x_1,x_2)\left(sh^2\alpha/ch\alpha + \rho(x_1,x_2)sin^2\beta/cos\beta\right) \approx$$

$$\approx -q_\nu(x_1,x_2)sh\alpha/2. \qquad \text{(A2.15)}$$

Appendix 3.

EIGEN VALUES $\nu_{E,H}$

Return to the dispersion equations for the ideal toroidal waveguide:

E_z modes: $p_\nu(\gamma a,\gamma a(1+\delta))=0;$ (A3.1)

H_z modes: $s_\nu(\gamma a,\gamma a(1+\delta))=0;$ (A3.2)

$\gamma^2 = k^2-k_z^2, \qquad \delta=(b-a)/a$

Consider a dependence of ν_E, a root of (6.1) and of ν_H, a root of (6.2), on the frequency $\omega=kc$, or, for simplicity, on the argument $x=\gamma a$.

If $\nu \neq \gamma a, \gamma b$, we can approximately solve dispersion equations (A3.1) and (A3.2) via (A2.3):

The dispersion equations can be rewritten via asymptotic formulas (A2.4) as

E_z modes: $Ai(y_1)Bi(y_2)-Ai(y_2)Bi(y_1)=0$, or $\dfrac{Ai(y_1)}{Bi(y_1)} = \dfrac{Ai(y_2)}{Bi(y_2)}$; (A3.3)

H_z modes: $Ai'(y_1)Bi'(y_2)-Ai'(y_2)Bi'(y_1)=0,$

or $\dfrac{Ai'(y_1)}{Bi'(y_1)} = \dfrac{Ai'(y_2)}{Bi'(y_2)};$ (A3.4)

$$y_1 = -\left(\frac{2}{\nu}\right)^{1/3}(\gamma a-\nu); \quad y_2 = -\left(\frac{2}{\nu}\right)^{1/3}(\gamma b-\nu) = -\left(\frac{2}{\nu}\right)^{1/3}(\gamma a(1+\delta)-\nu).$$

Fig.12(a,b) shows the functions $\dfrac{Ai(y)}{Bi(y)}$ and $\dfrac{Ai'(y)}{Bi'(y)}$.

1. $\nu < \gamma a, \gamma b$, i. e. $y_1, y_2 < 0$.

The Debye approximation (5.3) leads to next dispersion equations:

$$p_\nu(x_1,x_2)=0 \rightarrow \sin(\varphi_2-\varphi_1+(u_1-u_2)/\nu)=0 \Rightarrow$$

$$(\nu tg^2\beta+(1+5ctg^2\beta)/(8\nu sin^2\beta))ctg\beta=\pi n/\delta \Rightarrow \nu_E=\nu_0+\frac{1+5ctg^2\beta_0}{8\nu_0\ sin\beta_0};$$

$$s_\nu(x_1,x_2)=0 \rightarrow \sin(\varphi_2-\varphi_1+(v_2-v_1)/\nu)=0 \Rightarrow$$

$$(\nu tg^2\beta-(3+7ctg^2\beta)/(8\nu sin^2\beta))ctg\beta=\pi n/\delta \Rightarrow \nu_H=\nu_0-\frac{3+7ctg^2\beta_0}{8\nu_0\ sin\beta_0},$$

where $\nu_o=\left(x^2-(\pi n/\delta)^2\right)^{1/2}$, $\sin\beta_0=\pi n/\delta x$, $x_{1,2}=x(1\mp\delta/2)$ (A3.5)

If the curvature decreases, retaining $x\cdot\delta=const$, i. e. retaining $sin\beta_0=const$ and increasing x, then the difference between longitudinal wavenumbers for the curve waveguide (ν_E, ν_H) and for the straight one (ν_0) decreases as 1/x. If the curvature δ retains constant, the differences of the squares of the wavenumbers ($\nu_{E,H}^2-\nu_0^2$) decrease with increasing the modes number n.

2. $\gamma a<\nu<\gamma b$, i. e. $y_2 < 0 < y_1$.

Airy function for big positive arguments has exponential approximation [4] (10.4.(59, 61, 63, 66)),which leads to
E_z modes:

$$\mathrm{tg}\left(\frac{\pi}{4} + \nu(w_2-\mathrm{arctg}(w_2))\right)=M(y_1)\frac{1}{2}\exp\left(-2\nu(\mathrm{arth}(w_1)-w_1)\right),$$

H_z modes:

$$\mathrm{ctg}\left(\frac{\pi}{4} + \nu(w_2-\mathrm{arctg}(w_2))\right)=M(y_1)\frac{1}{2}\exp\left(-2\nu(\mathrm{arth}(w_1)-w_1)\right),$$

(A3.6)

where $w_2=\sqrt{(\gamma b/\nu)^2-1}$, $w_1=\sqrt{1-(\gamma a/\nu)^2}$, and M(y) is a slightly changing function: $M(0)=2/\sqrt{3}$, and $M(y)\approx 1$ for big arguments. The graphical solution in variables $y_{1,2}$ is shown in the fig.13. The figures 13a show a high frequency case,when E_z and H_z modes have a great number eigen values in the region $\gamma a<\nu<\gamma b$; the figures 13b - a case, when the delayed modes only begin to appear(one E_z and two H_z modes in this region); the figures 13c show a low frequency case, when the region $\gamma a<\nu<\gamma b$ contains the only H_z mode with eigen value $\nu\approx(\gamma a+\gamma b)/2$.

If we consider the waveguide with a small curvature $\delta=(b-a)/a\approx(\gamma b-\gamma a)/\nu \ll 1$, then, denoting $w_1=\mathrm{th}(\alpha)$ and $w_2=\mathrm{tg}(\beta)$, we can write:

$$\nu=\gamma b\cos\beta=\gamma a(1+\delta)(1-2\sin^2(\beta/2)) =$$
$$= \gamma a\,\mathrm{ch}\alpha=\gamma a(1+2\mathrm{sh}^2(\alpha/2)), \qquad \text{(A3.7)}$$

hence,

$$\mathrm{sh}^2(\alpha/2)+(1+\delta)\sin^2(\beta/2) = \delta/2,$$

or, for $\delta\ll 1$,

$$\alpha^2+\beta^2=2\delta. \qquad \text{(A3.8)}$$

Substituting (A3.7) and(A3.8) into (A3.6), we get the dispersion equation in a form $F_1(\alpha^2) = F_2(2\delta-\alpha^2)$ and, solving it relatively α, we find the eigen value ν. This procedure results with

$$\nu_E\approx y\left(1-\xi\left(C_{1E}/y\right)^{2/3}\right),\quad C^0_{1E}=\pi(l-1/4),\ l\geq 1;$$

$$\nu_H\approx y\left(1-\xi\left(C_{1E}/y\right)^{2/3}\right),\quad C^0_{1H}=\pi(l-3/4),\ l\geq 1;$$

$$C_l = C^0_l + \frac{1}{2}\exp\left(-\frac{2}{3}A\left(1-\left(3C^0_l/A\right)^{2/3}\right)^{3/2}\right)$$ for E_z or H_z modes.

where $\xi = 3^{2/3}/2 \approx 1.04$; $A=y(2\delta)^{3/2}$.

The roots of (A3.3) are close to the zeros of Ai, and the roots of (A3.4) - to the zeros of Ai'.

The fig.14 shows the dependence of the eigen values ν on the argument x for equations $p_\nu(x,x(1+\delta))=0$ and $s_\nu(x,x(1+\delta))=0$ ($\delta=0.2$). When $\nu<x$, the dispersion curves are close to the ones of a straight waveguide, the eigen values of E_z and H_z modes practically coincide. But when the argument increases, the dispersion curves not only approach to the line $\nu=x$, but cross this line and find themselves in the region $x<\nu<x(1+\delta)$. Here the eigen values of E_z and H_z modes differ essentially: ν_H are approximately in the middle between neighbour ν_E.

3. $|y_1|, |y_2| \ll 1$.

In this case we can use power series [4] (10.4.2, 10.4.3):

E_z modes: $Ai(y_1)Bi(y_2)-Ai(y_2)Bi(y_1)=0 \Rightarrow$

$(1+y_1^3/6+y_1^6/180)(y_2+y_2^4/12+y_2^7/504)-$

$-(1+y_2^3/6+y_2^6/180)(y_1+y_1^4/12+y_1^7/504)=0$

H_z modes: $Ai'(y_1)Bi'(y_2)-Ai'(y_2)Bi'(y_1)=0 \Rightarrow$

$(y_1^2/2+y_1^5/30)(1+y_2^3/3+y_2^6/72)-(y_2^2/2+y_2^5/30)(1+y_1^3/3+y_1^6/72)=0.$

We find that there are no E_z modes in this region, and there is one H_z mode with

$\nu_H \approx \gamma a(1+\frac{\delta}{2}(1+(\delta\gamma a)^3/(30\gamma a)))$, where $(\delta\gamma a)^3/(30\gamma a) \ll 1$. (A3.9)

At $y_{1,2} \to 0$ (i. e. for small curvature or small frequency) $\nu_H \to \gamma(a+b)/2$ and simultaneously coincides with the longitudinal straight waveguide wavenumber for the H_z mode with a zero x(r)-component of the wavenumber. That is why we have compared ν with the longitudinal wavenumber k_y with ν divided by the average camera radius $\langle r \rangle = (a+b)/2$.

Appendix 4

RESONANT PARAMETERS

1. Resonant frequencies.

The resonant frequency can be found from the equation:

$(k_{res}R/\beta)^2-\nu_0^2(k_{res})=0,$ (A4.1)

where

$\nu_0(k) \approx \gamma b\left(1-\xi\left(C_l/\gamma b\right)^{2/3}\right) \Rightarrow$

$\nu_0^2(k) \approx (k^2-k_z^2)b^2\left(1-2\xi\frac{C_l^{2/3}}{((k^2-k_z^2)b^2)^{1/3}}\right)$ (for $l \neq 0$). (A4.2)

Thus, the resonant frequency can be found as $k^2=\gamma^2+k_z^2=x^3/b^2+k_z^2$, where x is a root of the equation:

$x^3 - x^2\,(\xi C_l^{2/3}/\delta_r) - (\pi p/2\delta_z\beta)^2/2\delta_r = 0,$

where $\delta_r = R/\beta b - 1$; $\delta_z = g/R$.

For $p=0$ $(kb)^2=(\xi/\delta_r)^3 C_l$. (A4.3)

For $p \neq 0$ (A4.2) can be rewritten as

$y^3 - y^2\,A - 1 = 0,$ (A4.4)

where $y = x\,2\delta_r\left(2\beta\delta_z/\pi p\delta_r\right)^{2/3}$, $A = 2\xi\left(2\beta\delta_z C_l/\pi p\delta_r\right)^{2/3}$.

In two opposite cases we have the following approximations:

1) $A \gg 1 \Rightarrow y \approx A+1/A^2 = A(1+1/A^3)$,

$x^3=(y/2\delta_r)^3\left(\pi p\delta_r/2\beta\delta_z\right)^2 \approx (\xi/\delta_r)^3 C_l^2,$

$(kb)^2=x^3+(k_z b)^2 = (3C_l)^2/(2\delta_r)^3 + (\pi p/2\delta_z)^2.$ (A4.5)

2) $A \ll 1 \Rightarrow y \approx 1-A/3$,

$x^3 \approx (1/(8\delta_r)\left(\pi p/2\beta\delta_z\right)^2,$

$(kb)^2=x^3+(k_z b)^2 \approx (\pi p/2\delta_z)^2(1+1/(8\delta_r\beta^2)).$ (A4.6)

For $l=0$ $\nu_0^2(k)\approx(\gamma a)^2(1+\delta(1+\delta^3(\gamma a)^2/30))$, it gives

$$(kb)^2\approx(k_z b)^2+(\pi p/2\delta_z\beta)^2\,\frac{1+2\delta}{\delta+2\delta_r} \qquad \text{for } p\neq 0 \qquad (A4.7)$$

$$(kb)^2\approx 30(\delta+2\delta_r)(1+2\delta)/\delta^4 \qquad \text{for } p=0. \qquad (A4.8)$$

2. The widths of the resonances.

The resonant bands can be found from the condition of equal real and imaginary parts of the resonant factor.

a)Resonant band in r-direction.

$$\mathrm{Re}\left(\frac{2\nu}{(\omega R/\beta c)^2-\nu^2}\right)=\mathrm{Im}\left(\frac{2\nu}{(\omega R/\beta c)^2-\nu^2}\right) \Rightarrow \mathrm{Re}(\omega R/\beta c-\nu)=\mathrm{Im}(\omega R/\beta c-\nu)$$

$$\mathrm{Re}(\omega R/\beta c-\nu)=\omega R/\beta c-(\omega R/\beta c)_{res} = \Delta(\omega R/\beta c)=\nu_i,$$

$$\Delta r\approx \nu_i \beta c/\omega.$$

b)Resonant band in k-direction.

As ν depends on k as (A4.2),the resonant band can be found as:

$$\begin{cases}(k_{res}R/\beta)^2-\nu_0^2(k_{res})=0;\\ \mathrm{Re}\left((kR/\beta)^2-\nu_0^2(k)-2\nu_0\, i(k)\nu_i\right)=\mathrm{Im}\left((kR/\beta)^2-\nu_0^2(k)-2\nu_0 i(k)\nu_i\right),\end{cases}$$

$$2k\Delta k\frac{\partial}{\partial k^2}\left((kR/\beta)^2-\nu_0^2(k)\right)\Big|_{k_{res}}=2k\Delta k\frac{\partial}{\partial\gamma^2}\left((\gamma R/\beta)^2-\nu_0^2(\gamma)\right)\Big|_{k_{res}}=$$

$$= 2\nu_0(k_{res})\nu_i.$$

For $l\neq 0$

$$\frac{\partial}{\partial\gamma^2}\left((\gamma R/\beta)^2-\nu_0^2(\gamma)\right)\approx b^2\left((R/b)^2-\nu_0^2/(\gamma b)^2-\frac{2\xi C_l^{2/3}}{3(\gamma b)^{2/3}}\right)=$$

$$=\frac{1}{\gamma^2}\left(((Rk/\beta)^2-\nu_0^2)-(Rk_z/\beta)^2-\frac{2\xi C_l^{2/3}}{3(\gamma b)^{2/3}}\right)=$$

$$=-\frac{1}{\gamma^2}\left((\pi p/\beta 2\delta_z)^2+\frac{2\xi C_l^{2/3}}{3(\gamma b)^{2/3}}\right);$$

$$\Delta k=\frac{\gamma^2\, 2\nu_0(k_{res})\nu_i}{k\left((\pi p/2\beta\delta_z)^2+\frac{2\xi C_l^{2/3}}{3(\gamma b)^{2/3}}\right)}\approx\frac{\gamma^2\, 2(R/\beta)}{\left((\pi p/2\beta\delta_z)^2+\frac{2\xi C_l^{2/3}}{3(\gamma b)^{2/3}}\right)}\nu_i;$$

For $p\neq 0$, $l\neq 0$ $(\pi p/\beta\delta_z)^2\gg 1$ and $\xi\left(C_l/\gamma b\right)^{2/3}<\delta\ll 1$, thus we can write

$$\Delta k\approx\frac{\gamma^2 2(R/\beta)}{(\pi p/\beta 2\delta_z)^2}\nu_i;\ \Delta(kb)=\Delta(n)=2\nu_i\left((kb)^2/(\pi p/\beta 2\delta_z)^2-1\right).$$

For $p=0$, $l\neq 0$

$$\Delta k=\frac{\gamma^2\ (R/\beta)\ 3(\gamma b)^{2/3}}{\xi C_l^{2/3}}\nu_i \Rightarrow \Delta(kb)=\Delta(n)\approx 3\,\frac{(\gamma b)^{8/3}}{\xi C_l^{2/3}}.$$

$A\gg 1 \Rightarrow (kb)^2=(3C_l)^2/(2\delta_r)^3+(\pi p/2\delta_z)^2 \Rightarrow$

$$\Delta(n)=2\nu_i\frac{(3C_l)^2/(2\delta_r)^3}{(\pi p/2\delta_z)^2},$$

2)$A \ll 1 \Rightarrow (kb)^2 \approx (\pi p/2\delta_z)^2(1+1/(8\delta_r\beta^2)) \Rightarrow$

$\Delta(n) = 2\nu_i/(8\delta_r\beta^2)$.

For l=0

$$\frac{\partial}{\partial\gamma^2}\left((\gamma R/\beta)^2-\nu_0^2(\gamma)\right)=(R/\beta)^2-a^2(1+\delta(1+2\ \delta^3(\gamma a)^2/30));$$

$$\Delta(kb)=\Delta(n)=\frac{\nu_0(k_{res})\nu_i}{kb(2\delta_r+\delta)} \qquad (p\neq 0).$$

3. The shunt impedance.

The resonant peaks of E_z and H_z modes can be estimated as:

$$R_{shunt}=\left(\mathrm{Re}(Z_l(\omega)/n)\right)_{max}=$$

$$=-\mathrm{Re}\left[\frac{2\pi R}{k}\ \frac{\Lambda_p}{N_s}\ E^2_{s,\theta}(R_0)\ \sin^2(k_{zp}z_0+\pi p/2)\right]_{res}\cdot \mathrm{Im}\left(\frac{2\nu}{(\omega/\omega_o)^2-\nu^2}\right)\approx$$

$$\approx\left[\frac{2\pi R}{k}\ \frac{\Lambda_p}{N_s}\ E^2_{s,\theta}(R_0)\ \sin^2(k_{zp}z_0+\pi p/2)\right]_0\cdot\frac{1}{\nu_i},$$

where $\nu_i=\mathrm{Im}(\nu)$, and the index "0" at the term in square brackets means that it can be calculated assuming $\eta=0$.

Let the beam vertical position $z_0=0$, then, for the modes with $\Lambda_p\approx 1$ (see (3.17)) we have:

$$R_{shunt}\approx\left[\frac{2\pi R}{k}\ \frac{E^2_{s,\theta}(R_0)}{N_s}\right]_0\cdot\frac{1}{\nu_i},$$

$$N_s=\ 2\ \int\ [\vec{E}\times\vec{H}]d\vec{r}_\perp=\frac{-2\nu k}{\gamma_p^2 Z_0}\int\left(E_z^2+(Z_0H_z)^2\right)\frac{dr}{r}\cdot g(1\pm\delta_{0p})$$

(for E_z, H_z modes).

For $|\delta_r|=\delta/2$ and $A=2\xi\left(2\delta_z C_l/\pi p\delta_r\right)^{2/3}\gg 1$, $p,l\neq 0$ we have the next esteems.

$$ch^2\alpha_r=(\nu/(\gamma R))^2=(k/\gamma)^2=1+(k_z/\gamma)^2\Rightarrow$$

$$\alpha_r^2\approx(k_z/\gamma)^2\approx\delta\cdot(\pi p\delta/6\delta_z C_l)^2\ll\delta,\quad \alpha^2=\alpha_r^2+\delta\approx\delta.$$

$$\psi=\nu\alpha^3/3\approx C_l;\ \psi_r=\nu\alpha_r^3/3\approx C_l(\pi p\delta/6\delta_z C_l)^3$$

E_z modes:

$$\rho(\gamma_p b,\gamma_p a)\approx(\sin\beta/4sh\alpha)e^{2\psi}\gg 1$$

$$\frac{\partial p_\nu(\gamma_p b,\gamma_p a)}{\partial\nu}\approx -r_\nu(\gamma_p b,\gamma_p a)\cos\beta$$

$$\left|\frac{p_\nu(\gamma_p R_0,\gamma_p a)}{r_\nu(\gamma_p b,\gamma_p a)}\right|^2\approx(2e^{-\psi}sh(\psi-\psi_r))^2/(\alpha_r\beta)$$

$$N_s=\frac{-2\ k}{\gamma_p^2 Z_0}\ \frac{\gamma_p b}{2}\ r_\nu(\gamma a,\gamma b)\ \frac{\partial}{\partial\nu}p_\nu(\gamma a,\gamma b)\cdot g\approx\frac{kbg}{\gamma_p Z_0}\ r_\nu^2(\gamma b,\gamma a)/\cos\beta$$

$$R_{shunt}\approx\frac{(Z_0/\nu_i)\ 2\pi R/k}{kbg}\left(\frac{p_\nu(\gamma_p R_0,\gamma_p a)}{r_\nu(\gamma_p b,\gamma_p a)}\frac{k_z\nu}{R\gamma_p^2}\right)^2\gamma_p\cos\beta=$$

$$=\frac{2\pi Z_0}{(kb)\ \nu_i\delta_z}(2e^{-\psi}sh(\psi-\psi_r))^2(\alpha_r/\beta).$$

where $\nu_i=\mathrm{Re}(\eta)/\delta_z$, $C_l=(l-1/4)\pi$, $l\geq 1$.

H_z modes:

$$\rho(\gamma_p b,\gamma_p a)\approx 4(\sin\beta/\mathrm{sh}\alpha)e^{-2\psi} \ll 1$$

$$\frac{\partial s_\nu(\gamma_p b,\gamma_p a)}{\partial\nu}\approx q_\nu(\gamma_p b,\gamma_p a)\beta^2$$

$$\left|\frac{s_\nu(\gamma_p R_0,\gamma_p a)}{q_\nu(\gamma_p b,\gamma_p a)}\right|^2\approx\alpha_r\beta\ (2e^{-\psi}\mathrm{sh}(\psi-\psi_r))^2$$

$$N_s=\frac{2k}{\gamma_p^2 Z_0}\ \frac{\gamma_p b}{2}\ q_\nu(\gamma a,\gamma b)\ \frac{\partial}{\partial\nu}s_\nu(\gamma a,\gamma b)\cdot g\approx\frac{kbg}{\gamma_p Z_0}\ q_\nu^2(\gamma b,\gamma a)\beta^2$$

$$R_{\text{shunt}}\approx\frac{(Z_0/\nu_1)\ 2\pi R/k}{kbg}\left(\frac{s_\nu(\gamma_p R_0,\gamma_p a)k}{q_\nu(\gamma_p b,\gamma_p a)\ \gamma_p}\right)^2\gamma_p/\beta^2=$$

$$=\frac{2\pi Z_0}{(kb)\ \nu_i\delta_z}(2e^{-\psi}\mathrm{sh}(\psi-\psi_r))^2(\alpha_r/\beta).$$

where $\nu_i=\mathrm{Re}(\eta)/\delta$, $C_l=(l+1/4)\pi$, $l\geq 1$.

If $\alpha_r^2/\delta\ll 1$, hence $\psi\gg\psi_r$, $\beta\approx\delta^{1/2}$, $\gamma\approx k$, and (for $\psi\geq 1$)

$$R_{\text{shunt}}\approx\frac{\pi^2 Z_0 p}{(kb)^2\nu_i\delta_z^2\delta^{1/2}}$$

where ν_i for E_z and H_z modes are given above.

References

1. *R. Warnock, P. Morton.* Fields excited by a beam in a smooth toroidal chamber. SLAC-PUB-4562, 1988.
2. *K.Y. Ng.* Resonant impedance in a toroidal beam pipe. SSC-163/FN-477, 1988.
3. *K.Y. Ng, R. Warnock.* Reactive impedance of a smooth toroidal chamber below the resonance region. Phys.Rev.D, vol.40, N 1, p.231, 1989.
4. *M. Abramowitz, I.A. Stegun.* Handbook of mathematical functions.
5. *Erdelyi A. et al.* Higher transcendental functions. McGrav-Hill Book Co., 1953,V2, Ch.7.
6. *L.A. Vainstein.* Electromagnetic waves. Moscow, 1988.

List of figures.

Fig.1. Toroidal chamber cross section with denotations.
Fig.2. Functions p_ν, q_ν, s_ν.
Fig.3. Berkley storage ring. Vertical walls with finite conductivity. Radial and vertical dependence of the impedance of the straight and curve waveguide in the subresonant region; vertical walls with finite conductivity; a,b - impedances of the straight and curve waveguide; c,d - their difference.
Fig.4. The same for the horizontal walls with finite conductivity (Berkley storage ring. Radial and vertical dependence of the impedance of the straight and curve waveguide in the subresonant region; horizontal walls with finite conductivity; a,b - impedances of the straight and curve waveguide; c,d - their difference.)
Fig.5. Berkley storage ring. Radial dependence of the impedance in the resonant region:
a)vertical walls with finite conductivity;
b)horizontal walls with finite conductivity.
Fig.6. Berkley storage ring. Frequency dependence of the impedance in the resonant region:
a)vertical walls with finite conductivity;
b)horizontal walls with finite conductivity;
c)all four walls with finite conductivity.
Fig.7. Phi-factory. Frequency dependence of the impedance. All four walls with finite conductivity.
Fig.8. Phi-factory. Radial dependence of the impedance. All four walls with finite conductivity. Zero width of a beam.
Fig.9. Resonant peak for different radial beam dimensions.
Fig.10. Shunt impedance dependence on the radial beam dimension.
Fig.11. Phi-factory. Frequency dependence of the impedance. All four walls with finite conductivity. Nonzero radial beam dimension.
Fig.12(App). Functions Ai/Bi, Ai'/Bi'.
Fig.13(App). A picture of the dispersion equation solution.
Fig.14(App). Eigen values dependence on the frequency.

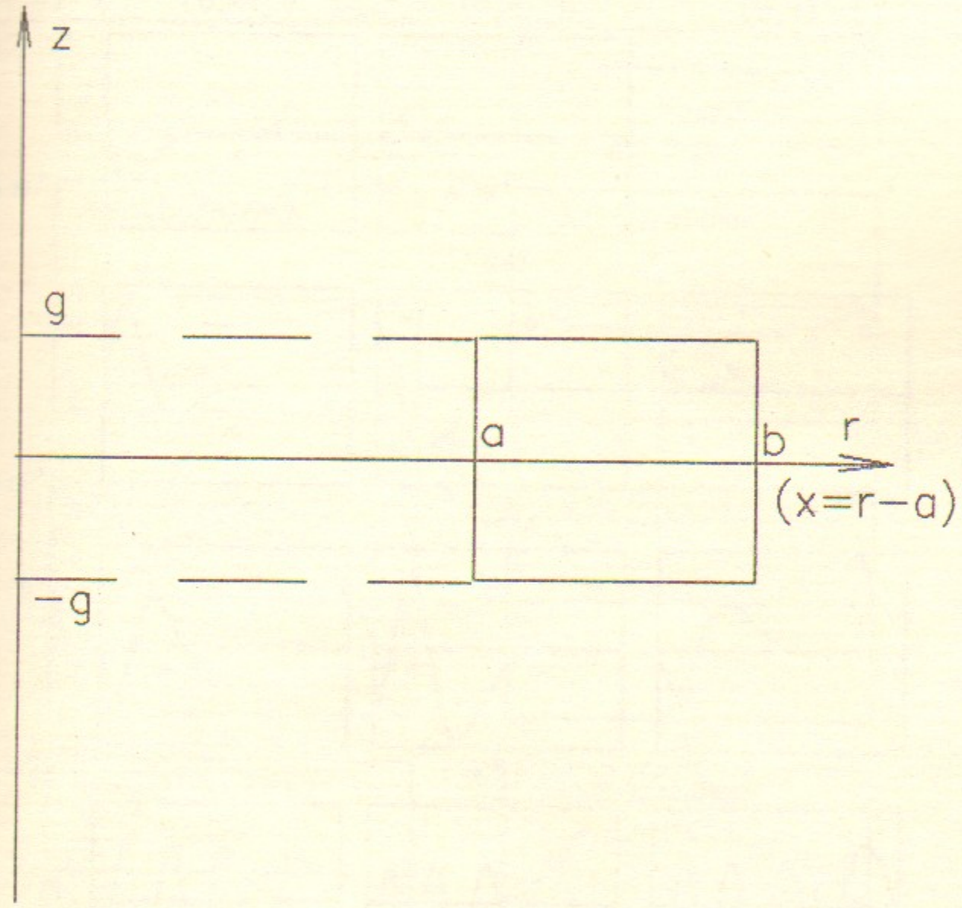

Fig.1

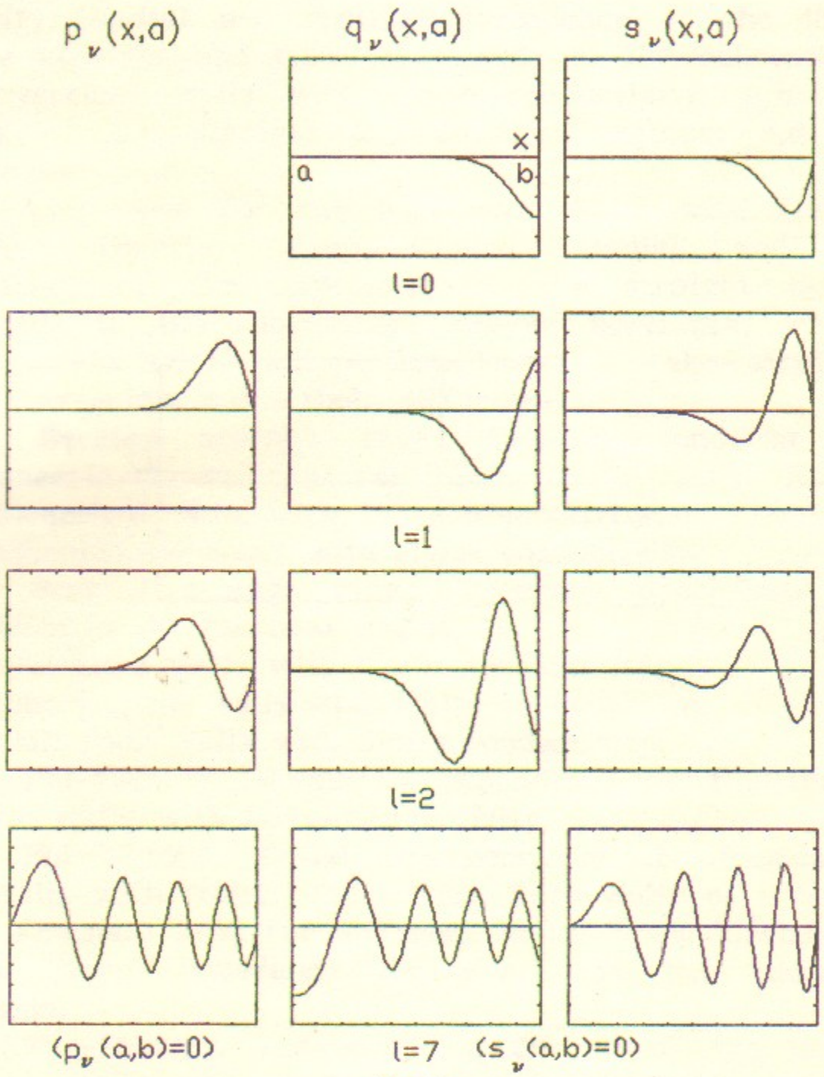

Fig.2

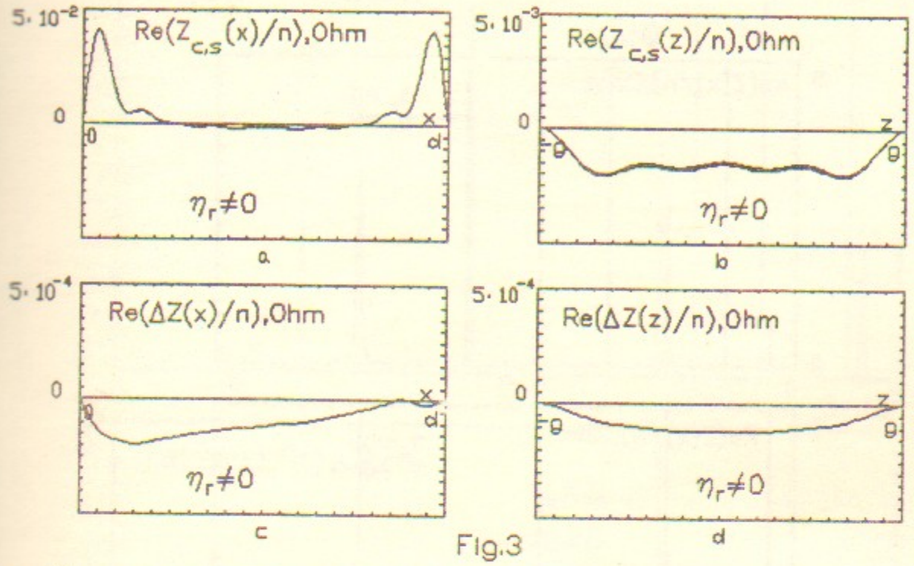

Fig.3

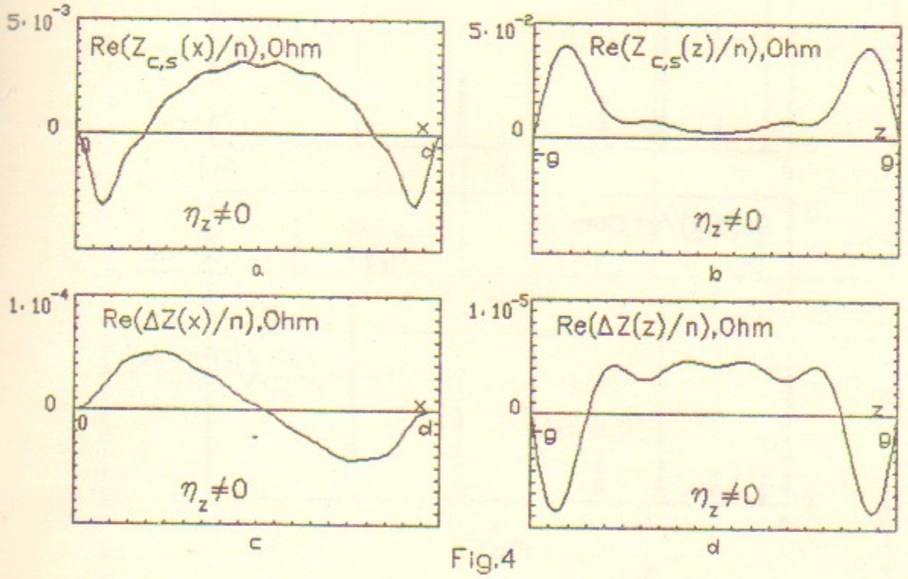

Fig.4

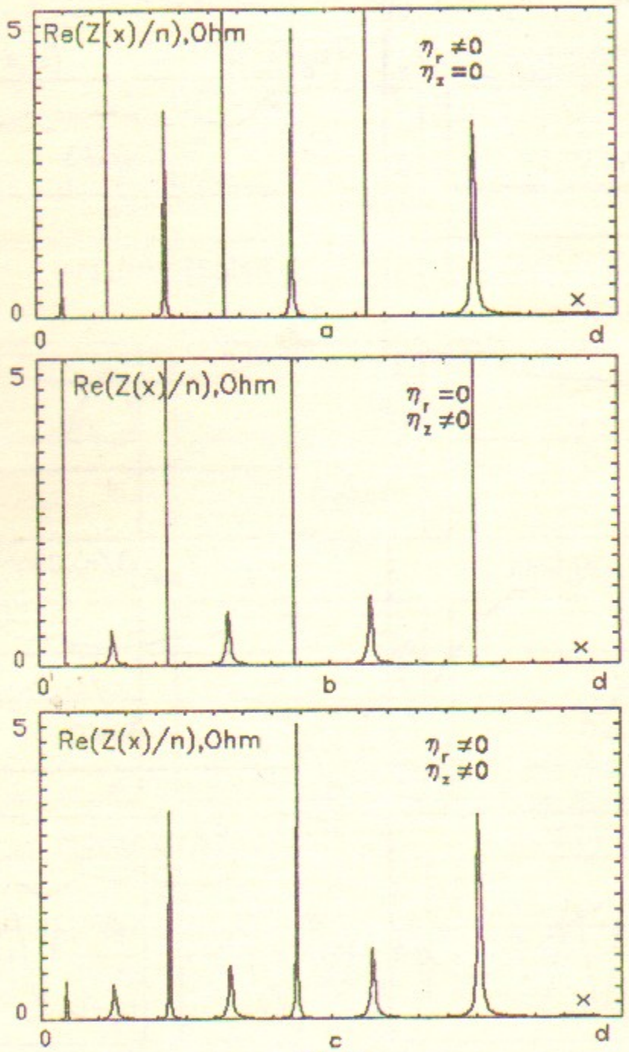
5
Re(Z(x)/n),Ohm
$\eta_r \neq 0$
$\eta_z = 0$
0
0
a
d
×
5
Re(Z(x)/n),Ohm
$\eta_r = 0$
$\eta_z \neq 0$
0
0'
b
d
×
5
Re(Z(x)/n),Ohm
$\eta_r \neq 0$
$\eta_z \neq 0$
0
0
c
d
×

Fig.5

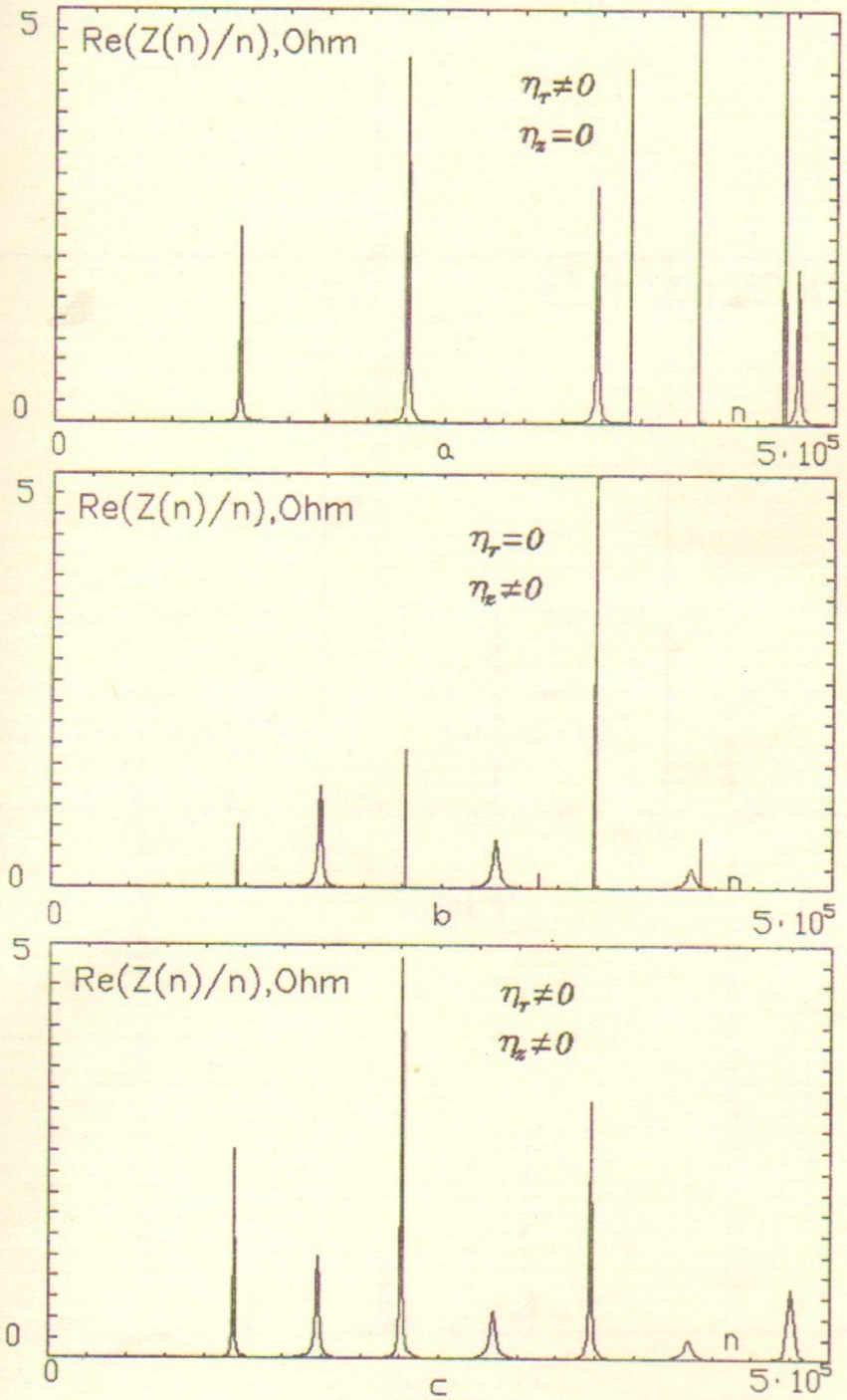
5
Re(Z(n)/n),Ohm
$\eta_r \neq 0$
$\eta_z = 0$
0
0
a
$5 \cdot 10^5$
n
5
Re(Z(n)/n),Ohm
$\eta_r = 0$
$\eta_z \neq 0$
0
0
b
$5 \cdot 10^5$
n
5
Re(Z(n)/n),Ohm
$\eta_r \neq 0$
$\eta_z \neq 0$
0
0
c
$5 \cdot 10^5$
n

Fig.6

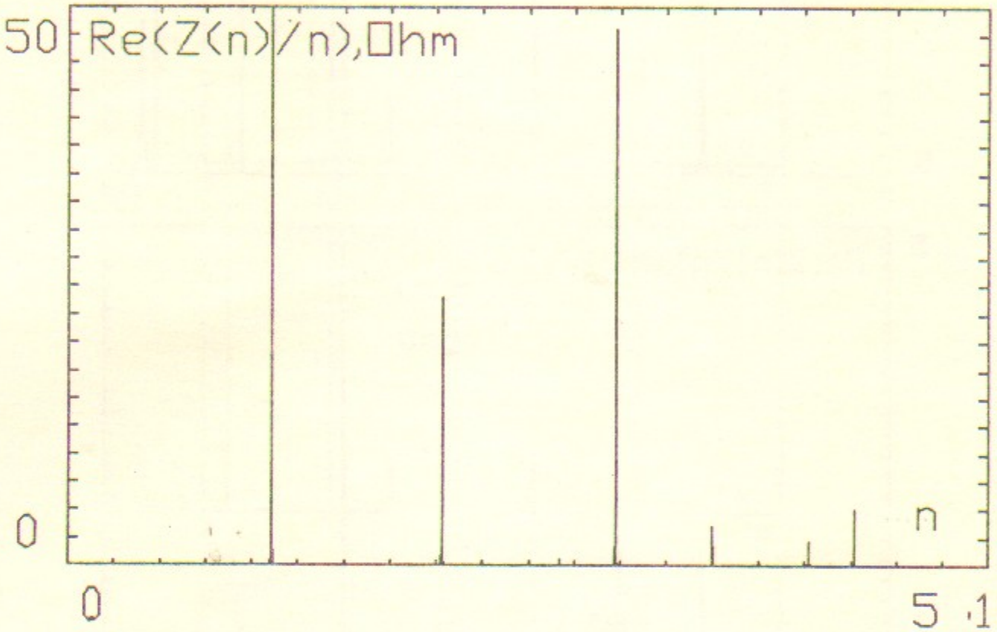
50
Re(Z(n)/n),Ohm
0
n
0
5 ·10⁴

Fig.7

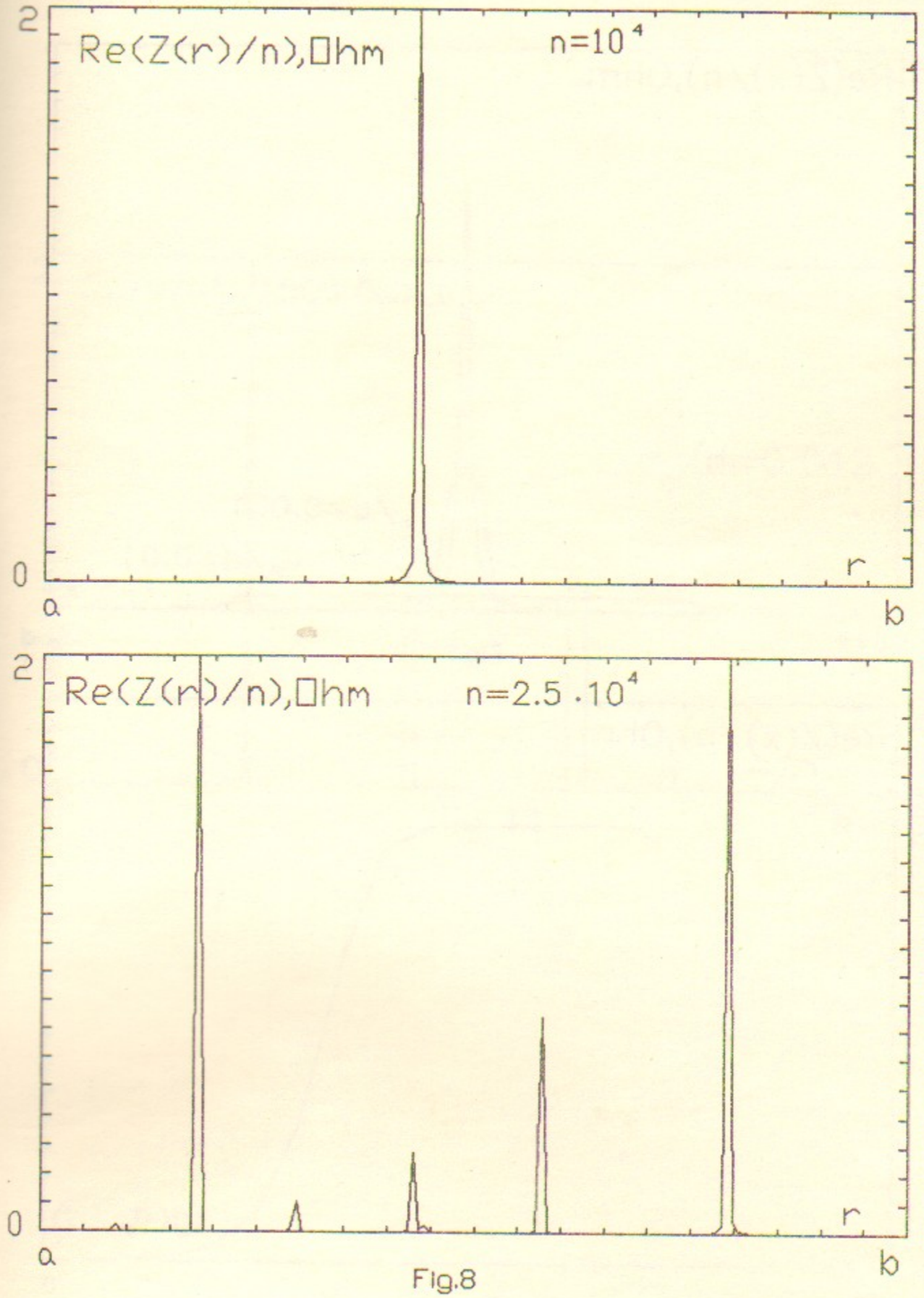
2
Re(Z(r)/n),Ohm
n=10⁴
0
r
a
b
2
Re(Z(r)/n),Ohm
n=2.5 ·10⁴
0
r
a
b

Fig.8

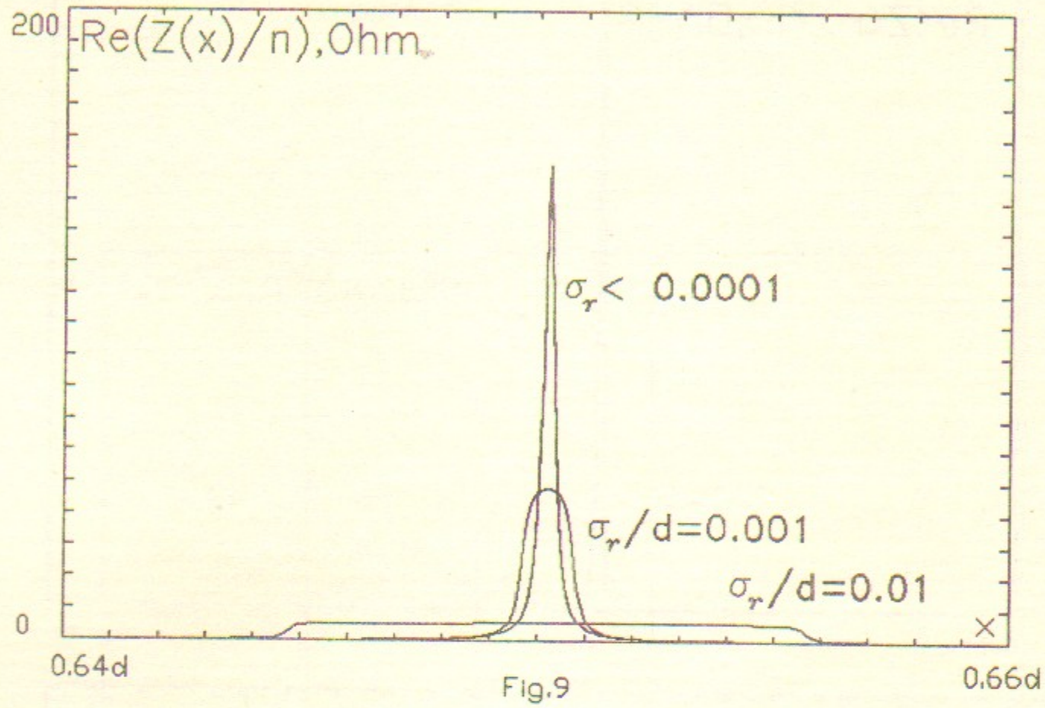

Fig.9

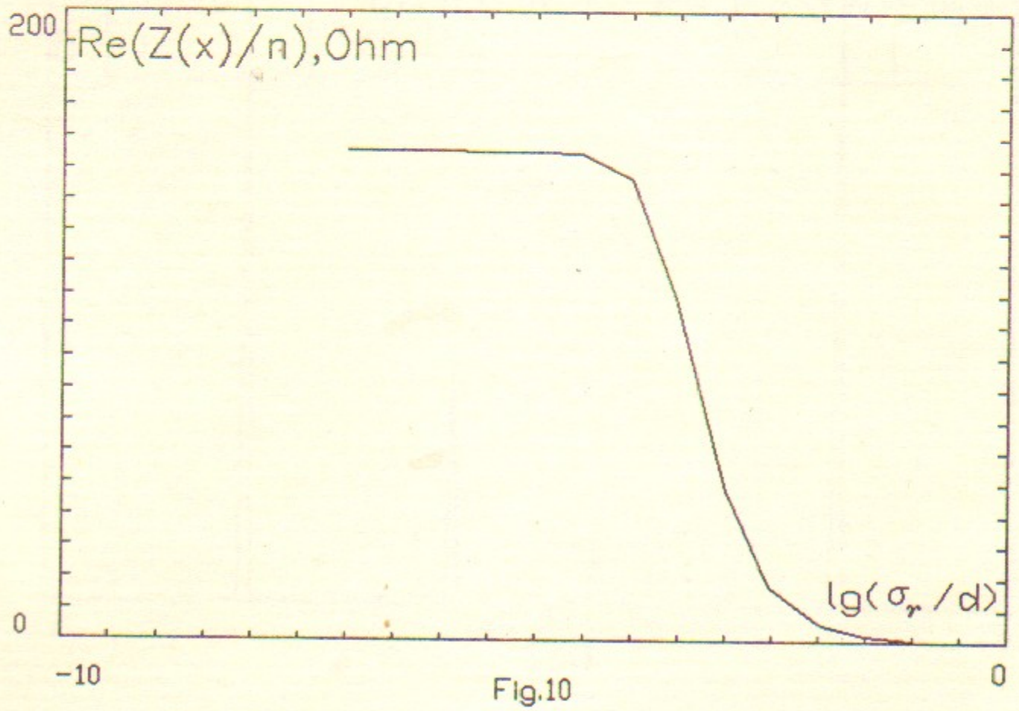

Fig.10

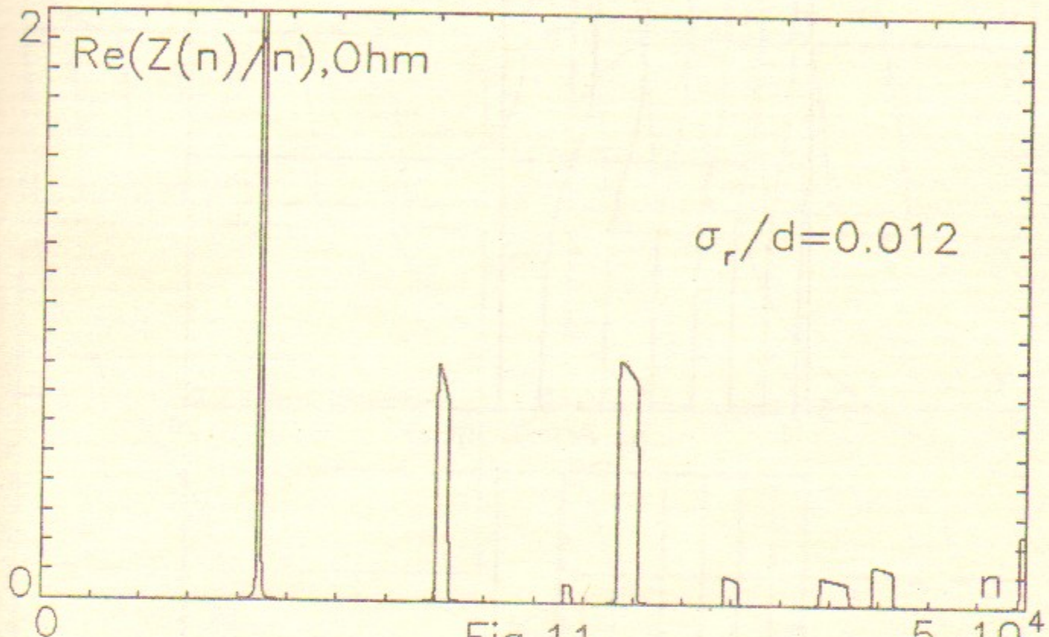

Fig.11

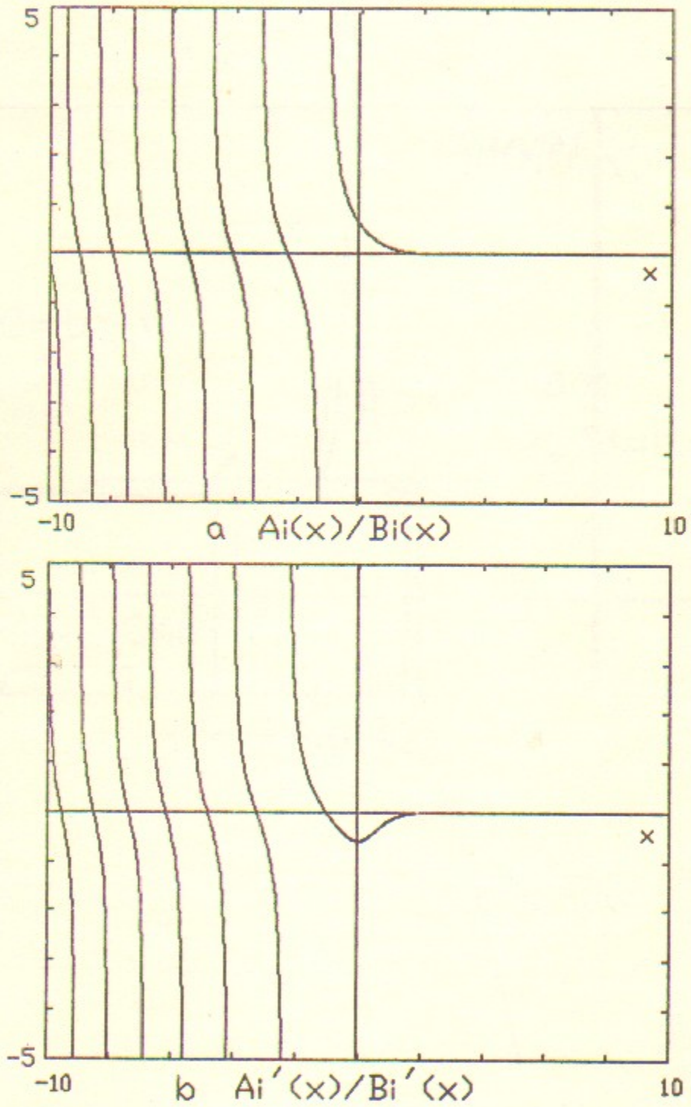

Fig.12

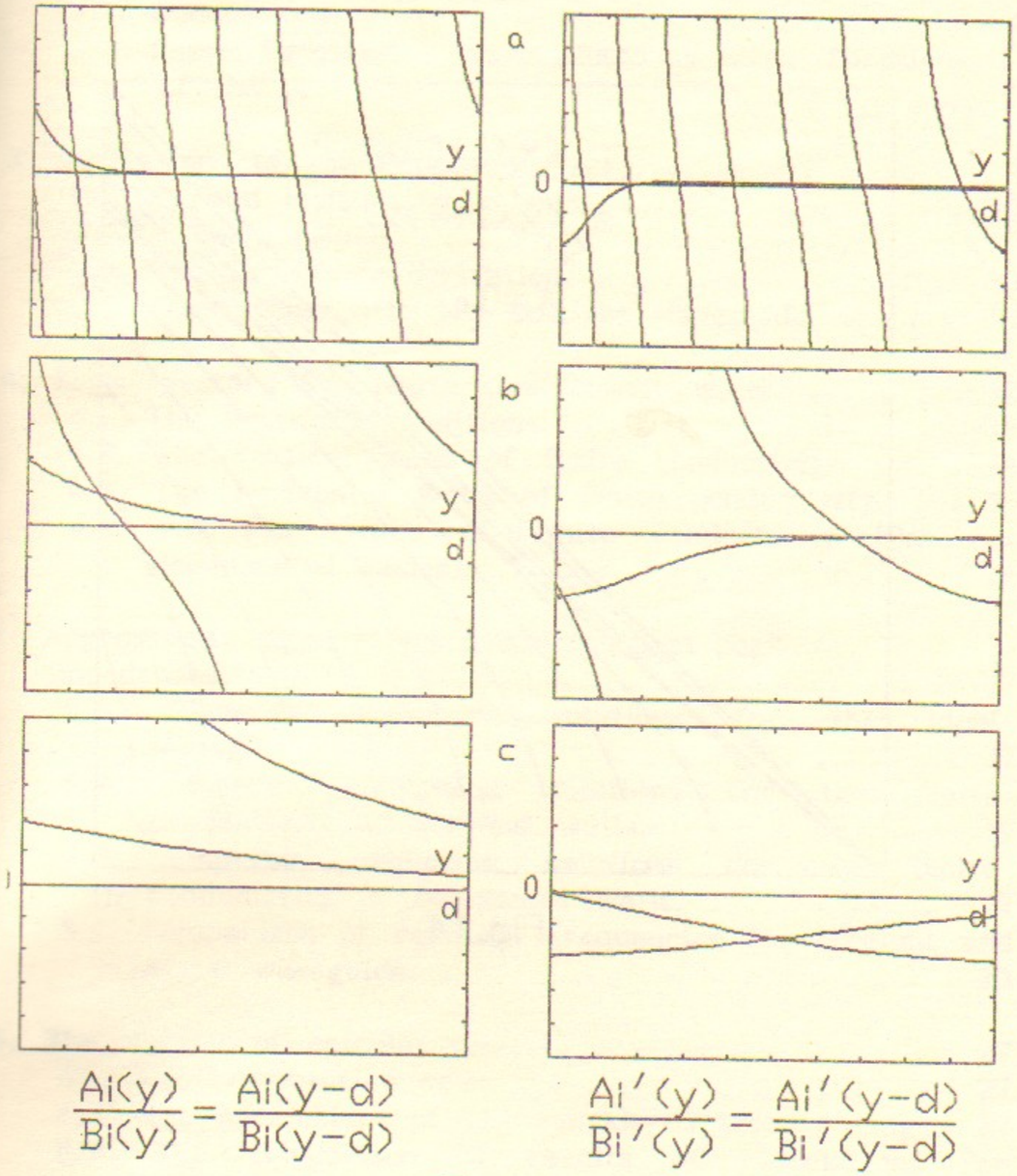

$$\frac{Ai(y)}{Bi(y)} = \frac{Ai(y-d)}{Bi(y-d)} \qquad \frac{Ai'(y)}{Bi'(y)} = \frac{Ai'(y-d)}{Bi'(y-d)}$$

Fig.13

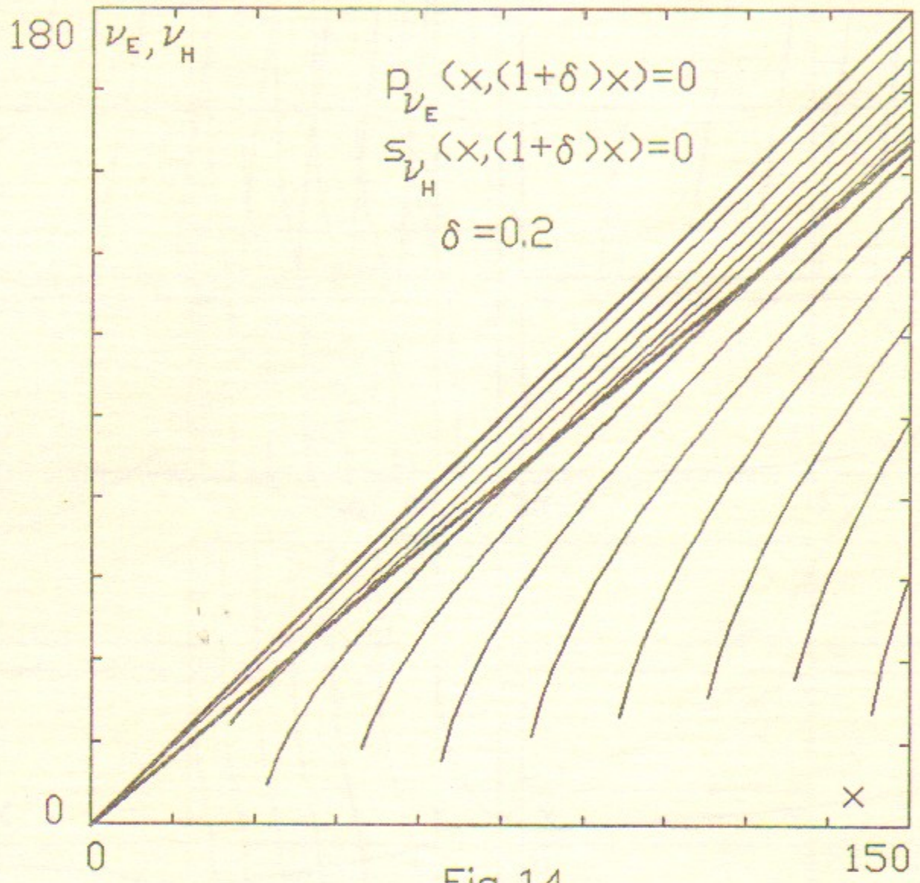

Fig.14

Contents.

1. Introduction. 3

2. Eigen functions for a curve waveguide. 4
   2.1. Denotations. 4
   2.2. Bessel functions cross-products as eigen functions of the problem. 5

3. Derivations of the impedance. 7
   3.1. A field induced by a beam. 7
   3.2. A beam model. 8
   3.3. The impedance derivation. 10
   3.4. Comparison with the straight waveguide. 11

4. Eigen vectors for finite conductivity walls. 12
   4.1. The boundary conditions. 12
   4.2. The vertical walls of finite conductivity. . . . 14
   4.3. The horizontal walls of finite conductivity. . . 16
   4.4. All four walls of finite conductivity (for not degenerated modes). 16

5. Approximate eigen values ν and resonant peak impedances. 17
   5.1. Dispersion equation solutions for the ideal waveguide. 17
   5.2. Dispersion equation solutions for the finite conductivity of vertical walls. 19
   5.3. Dispersion equation solutions for the finite conductivity of horizontal walls. 21
   5.4. Comparison of resonant frequencies for straight and curve waveguide. 23

6. The results of calculations. 27
   6.1. The computation code. 27
   6.2. The parameters of the considered storage rings.. 27
   6.3. The comparison of results of calculations for Berkley storage ring with results of Warnock [1]. 28

6.4. The results of calculations for a non-circular storage ring with big curvature. 30

7. Finite radial dimension of a beam. 32

8. Estimation formulas for resonant parameters. 35

Appendixes
1. Integrals of Bessel functions cross-products. 37
2. Approximation via Airy functions for J, Y and their derivatives. 37
3. Approximate values ν. 42
4. Resonant parameters. 46

References. 53
List if figures. 54

M.M. Karliner, N.V. Mityanina, V.P. Yakovlev

The Impedance of a Toroidal Chamber with Walls of Finite Conductivity. Waveguide Model

М.М. Карлинер, Н.В. Митянина, В.П. Яковлев

Импеданс тороидальной камеры с конечной проводимостью стенок. Волноводная модель

Работа поступила 27 октября 1993 г.

Подписано в печать 27.10.1993 г.
Формат бумаги 60×90 1/16 Объем 3,3 печ.л., 2,6 уч.-изд.л.
Тираж 200 экз. Бесплатно. Заказ N° 90

Обработано на IBM PC и отпечатано на
ротапринте ИЯФ им. Г.И. Будкера СО РАН,
Новосибирск, 630090, пр. академика Лаврентьева, 11.